NASA Technical Memorandum 85794

NASA-TM-85794 19840018314

Noise Generated by a Propeller in a Wake

P.J.W.Block

May 1984

NASA
National Aeronautics and
Space Administration

Langley Research Center
Hampton, Virginia 23665

DISPLAY 22/2/1

84N26382*# ISSUE 16 PAGE 2553 CATEGORY 71 RPT#: NASA-TM-85794 NAS 1.15:85794 84/05/00 65 PAGES UNCLASSIFIED DOCUMENT

UTTL: Noise generated by a propeller in a wake

AUTH: A/BLOCK, P. J. W.

CORP: National Aeronautics and Space Administration. Langley Research Center, Hampton, Va. AVAIL.NTIS SAP: HC A04/MF A01

MAJS: /*AERODYNAMIC NOISE/*AIRCRAFT NOISE/*AIRCRAFT WAKES/*PROPELLER EFFICIENCY /*PROPELLERS

MINS: / AIRFOILS/ ANECHOIC CHAMBERS/ CHORDS (GEOMETRY)/ NEAR FIELDS/ NOISE MEASUREMENT/ WIND TUNNEL TESTS

ABA: Author

ABS: Propeller performance and noise were measured on two model scale propellers operating in an anechoic flow environment with and without a wake. Wake thickness of one and three propeller chords were generated by an airfoil which spanned the full diameter of the propeller. Noise measurements were made in the relative near field of the propeller at three streamwise and three azimuthal positions. The data show that as much as 10 dB increase in the OASPL results when a wake is introduced into an operating propeller. Performance data are also presented for completeness.

ENTER:

TABLE OF CONTENTS

INTRODUCTION

As more economical and energy efficient air transportation is sought, propellers have become a prime candidate for the propulsion systems of future transports. Among the many options for integrating these propellers with the airframe, "pusher" installations have been shown to offer many advantages. These advantages stem from cost, weight, and/or aerodynamic considerations. Unfortunately, little data are available on the noise produced by a pusher installation. Such data are needed for developing and/or validating methods by which the noise impact of pusher propellers can be assessed.

Although many wind tunnel studies have been conducted on pusher propeller configurations, none were found containing noise measurements with which to guide this study. One full-scale flight test (ref. 1) of a pusher/tractor aircraft indicated that the pusher configuration was noisier than the tractor, but the data set was not sufficient to determine the characteristics of the noise. This current paper presents data obtained from an experimental study of the noise produced by a propeller operating in an airfoil wake.

Propeller performance and noise were measured on two model scale propellers operating in an anechoic flow environment with and without a wake. Wake thicknesses of one and three propeller chords were generated by an airfoil which spanned the full diameter of the propeller. Noise measurements were made in the relative near field of the propeller at three streamwise and three azimuthal positions. The data show that as much as a 10 dB increase in the OASPL results when a wake is introduced into an operating propeller. Performance data are also presented for completeness.

SYMBOLS AND ABBREVIATIONS

a_n, b_n, c_n	Fourier coefficients
c	chord of the propeller blade
C_D	propeller section drag coefficient
C_L	propeller section lift coefficient
C_P	power coefficient = $P/\rho n^3 d^5$
C_T	thrust coefficient = $T/\rho n^2 d^4$
d	propeller diameter
f	frequency
J	propeller advance ratio, U/nd
M	Mach number
M_T	helical tip Mach number
n	number of revolutions per second
P	power absorbed by the propeller
q	free-stream dynamic pressure
t	thickness of the wake
T	propeller thrust
T_A	air temperature
t	thickness of the airfoil wake
U	tunnel velocity
x_1, x_2, x_3	coordinates of the microphones with respect to the centerline of the propeller disk
α	angle of attack or pitch angle of the propeller axis with respect to the airstream
$\beta_{.75}$	propeller pitch setting at .75 radial station with respect to the plane of rotation
η	propeller efficiency
θ	orientation angle of the microphone with respect to the propeller disk plane

ϕ	orientation angle of the microphone with respect to the plane of the wake
ρ_A	air density

Abbreviations

OTS	open test section
mic	microphone
rev	revolution
dB	decibels
BPF	blade passage frequency
rpm	revolutions per minute
ips	inches per second
μPa	micropascals

DESCRIPTION OF THE EXPERIMENT

Test Apparatus and Facility

Propellers.- The two propellers tested were three-bladed, .25 scale propellers designed for the same twin engine airplane. In this report the two designs are designated Twin 1 and Twin 3. They were both 2.21 feet (.674 m) in diameter. Their chord and twist distributions and airfoil sections are given in figures 1 and 2. Twin 1 has Clark Y airfoil sections inboard and modified NACA 16 series sections outboard (fig. 1(b)). Twin 3 has ARA-D sections (fig. 2(b)). The two propeller designs are similar. The most notable difference is the airfoil sections employed. In particular Twin 3 has a much larger leading edge radius. Both propellers were fabricated from aluminum using three- and five-axis numerically controlled milling machines. They were dynamically balanced. When set in their respective hubs, the propeller pitch settings were adjustable in 0.5° increments and were secured by a locking pin. The pitch angle, $\beta_{.75}$, was read at the 75 percent radial position by resting an inclinometer flat against the lower surface. With this arrangement the pitch angle readings were accurate to 0.5° and were repeatable. The propeller section data were then used to determine the actual geometric angle of the chord line with respect to the plane of rotation.

Propeller Test Stand (PTS).- The PTS nacelle is a cylindrically shaped shell with a maximum outside diameter of 9 inches (.229 m) and overall length of 76 inches (1.93 m). It houses a quiet 50 hp, water cooled, synchronous electric motor which has a maximum speed of 8000 rpm. The motor turned the propellers clockwise looking upstream. The PTS was mounted vertically above a 4-foot (1.22-m) diameter circular jet which simulated the forward velocity for the propellers. A more complete description of the PTS and its operation in the Quiet Flow Facility is given in reference 2.

Quiet Flow Facility (QFF).- The QFF, located at the NASA Langley Research Center, is a large anechoic room with a very low turbulence quiet flow supply. A complete description of the flow and anechoic characteristics of the QFF is given in reference 3. In this test the low pressure air system provided the forward velocity through a 4-foot (1.22-m) diameter vertical jet. The maximum exit velocity of the jet was 120 fps (36.6 m/s). A schematic of the PTS in the QFF showing its location and other appropriate dimensions is given in figure 3. The nose of the spinner of the PTS was 30.25 inches (.77 m) above the exit of the jet. The position and flow characteristics of the potential core and shear layer with an operating propeller are documented in reference 2. The test matrix was designed to allow sufficient potential core between the propeller tips and the shear layer so that no correction to the propeller force data was required.

Wake producing airfoil.- To introduce a wake or velocity defect region into the propeller, a NACA 0020 airfoil was used. This airfoil was placed just upstream of the propeller and spanned the 4-ft jet. A photo of the airfoil upstream of the propeller is shown in figure 4. The two airfoils behind the propeller were not used during these tests. The angle of attack of the wake producing airfoil was manually adjustable. An angle of 15° was used to produce the narrower wake which was one propeller chord thick ($t/c \approx 1$). At an angle of 20.4° the flow over the airfoil was fully separated and the wake thickness was measured to be three propeller chords thick ($t/c \approx 3$). These wake thicknesses were chosen to provide the data necessary to validate a quasi-steady noise prediction method although no predictions are presented in this paper. The measurements of the velocity defect region produced by the airfoil are given in a later section. Figure 5 shows the dimensions and relative position of the airfoil with respect to the propeller disk. The airfoil position was shifted when its

angle of attack was changed so that the center of the wake would be a diameter of the circle representing the propeller disk. A secondary effect of the airfoil was to turn the flow coming into the propeller disk. No measurements were made to determine how much or how uniformly the flow was turned.

Microphone locations.- Noise measurements were made inside and outside of the flow at the microphone locations shown in figure 6. The measurements were made in the propeller plane (θ=0°) and 30° upstream (θ=-30°) and downstream (θ=+30°) from the propeller plane. Microphone 3, the only inflow microphone, was 1/4-inch (6.35 mm) in diameter and had a bullet-shaped nose. It was held in the flow by a specially designed rigid streamlined holder and by an adjustable stand. This microphone was positioned to as many as six locations for a given condition. The closest of these positions was 4.75 inches (.121 m) or .18 propeller diameters from the tip of the propeller. Microphones 4, 5, and 6 were located on a fixed stand outside the flow. These microphones were 1/2 inch (12.7 mm) in diameter and had a simple protective grid cap. The closest of these positions was the in-plane microphone (mic 5) which was 23.35 inches (.593 m) or .881 propeller diameters from the tip.

When the wake producing airfoil was upstream of the propeller, microphone 3 was positioned at the three streamwise locations (θ=-30°, 0°, +30°) for each of two azimuthal locations ϕ=25° and 90°. The azimuthal angle ϕ is the angle measured from the wake producing airfoil as shown in figure 6. The fixed stand holding microphones 4, 5, and 6 was oriented 77° from the plane of the airfoil. All microphone locations are given in Table 1 in terms of the coordinate system shown in figure 7. The distances from the center of the disk plane are also given in Table 1.

Test Conditions

The test had two parts: propeller performance measurements and propeller noise measurements. The conditions for the performance measurements are given in Table 2; for the noise measurements in Table 3. All tests were conducted at a forward speed of 120 fps (36.6 m/s).

The performance measurements (Table 2) were conducted over a series of rotational speeds for each blade pitch angle and inflow condition. The checks in Table 2 indicate conditions where a series of propeller performance measurements were made; the asterisks indicate the conditions where noise measurements were made.

The conditions for the noise measurements are expanded and given in Table 3. These tests were conducted at one rotational speed corresponding to a desired thrust setting. Both propellers were tested at thrust levels of 40 lbf (178 N) and 83 lbf (369 N). Twin 3 was also tested at 100 lbf (445 N). The measured values of the air temperature, propeller rpm, and thrust are given in Table 3 along with the computed values for the air density and for C_T, Cp, J, and M_T.

Measurements and Data Reduction

Propeller force data.- The propeller thrust was measured by a load cell located aft of the motor and grounded to the case (see ref. 2). The torque was measured by an in-line rotating shaft torque sensor which was isolated by two decouplers. The data from these sensors were read by a computer and stored on a disk.

The data were acquired beginning at an rpm which gave a minimum of 5 lbf (22.3 N) of thrust. The balance results were sampled about every 200 rpm until the maximum rpm or motor torque was reached. Then the rpm was decreased in about 200 rpm steps to the beginning rpm value.

The repeatability test cases showed that the thrust and power coefficient variation was less than .004.

The propeller operating conditions (C_T/J^2) were evaluated to ensure that the free jet contraction (due to the propeller operation) did not require a correction to the force data (see ref. 2). Any data requiring such a correction were purged from the data base and are not presented in this report.

The propeller performance data are presented in terms of the thrust and power coefficients (C_T, C_P) and the efficiency (η). Normally these coefficients are plotted against the advance ratio, $J = U/nd$. In these tests, however, the airfoil introduced a flow angle of attack into the propeller disk. In these cases the inflow velocity to the disk is $U \cos\alpha$ where α is the angle of the inflow with respect to the propeller axis. The inflow angle is assumed to be the angle of the wake producing airfoil. Thus, the performance data are plotted against $J \cos\alpha$ instead of J, with the efficiency being calculated as:

$$\eta = \frac{C_T}{C_P} J \cos\alpha$$

Wake data.- The airfoil wake was surveyed at the propeller plane to determine its position and thickness. (The propeller was not mounted on the PTS during these tests.) This was done using a pitot-static tube whose position was controlled by computer through a stepping motor. These data had a twofold purpose. First, the wake thickness was used to determine what airfoil angle of attack was necessary to produce a wake which was one propeller chord thick (t/c = 1) and three propeller chords thick (t/c = 3). These angles were 15° and 20.4° respectively. Second, the wake survey data were used to position the airfoil so that the centerline of the wake would be a diameter of the propeller disk.

The data were normalized by the free-stream dynamic pressure. The results for angles of attack of 15° and 20.4° are given in figure 8.

Noise data.- The propeller noise data were obtained both in the flow and out of the flow at the microphone locations given previously. During the test the acoustic data were recorded at 30 ips on one-inch magnetic tape for post-test analysis. The recording included a once-per-revolution signal from the shaft of the PTS which was used to accurately measure the rotational speed. The analysis proceeded as follows. Each data channel was sampled at 80,000 Hz along with the once-per-rev signal. The latter signal was used to document the period of the noise signal for each revolution of data. A harmonic analysis of each revolution was done which yielded the Fourier coefficients a_n and b_n where n is the number of the harmonic of the blade passage frequency. The Fourier coefficients were averaged for each revolution to produce $\bar{a}_n$ and $\bar{b}_n$. From these the magnitude of the noise component at each harmonic was computed using

$$c_n = \sqrt{\bar{a}_n^2 + \bar{b}_n^2} \quad .$$

These values were then converted to dB (re 20 μPa). This procedure was used to enhance the periodic components of the propeller noise signal while reducing the contribution of the random components via the averaging process. The random components are defined as those which are not related to the passage of the propeller blades such as the wake noise of the airfoil.

All the noise data are contained in this paper. Their presentation includes sample pressure time histories and averaged harmonic analyses. The computed overall sound pressure level, OASPL, and the blade passage frequency, BPF, are given with these data.

DATA RESULTS

Some of the data presented herein was previously published in reference 4. All of the measured performance and noise data are given in this report.

Performance Data

The performance data for the conditions listed in Table 2 were fit with a third order polynomial for ease of comparison and identification of trends and are presented in the figures of Appendix A.

Noise Data

All of the noise data measured with and without the wake producing airfoil are presented in the figures of Appendix B. The data are presented in the order given in the table of test conditions for the noise measurements, Table 3. Within each condition the data are presented for the upstream microphone followed by the in-plane and the downstream microphone. All the data for the inflow microphone locations is presented followed by that for microphones 4, 5, and 6.

The sample time histories reveal the following general characteristics. Upstream of the propeller disk negative spikes are introduced at the introduction of the wake. These most likely arise from the suction peak which develops as the blade encounters the wake. Downstream, positive peaks appear. At the lower disk thrust loadings both positive and negative spikes are observed.

The harmonic analyses of these time histories show the high harmonic content produced by these spikes. The t=3c cases tend to have the higher level fundamental and OASPL. The t = c cases often produce the higher levels in the higher harmonics particularly at the lower disk loading.

REFERENCES

1. Connor, A. B., Hilton, D. A., and Dingeldein, R. C.: Noise Reduction Studies for the Cenna Model 337 (O-2) Airplane. NASA TM X 72641, Apr. 1975.

2. Block, P. J. W.: Operational Evaluation of a Propeller Test Stand in the Quiet Flow Facility at Langley Research Center. NASA TM 84523, Sept. 1982.

3. Hubbard, H. H., and Manning, J. C.: Aeroacoustic Research Facilities at NASA Langley Research Center. NASA TM 84585, Mar. 1983.

4. Block, P. J. W., and Martin, R. M.: Results from Performance and Noise Tests of Model Scale Propellers. SAE Paper No. 830730, Apr. 1983.

Table 1.- Microphone Coordinates

Mic. No.	Coordinate in inches (m)			Distance	Relative position with respect to	
	x_1	x_2	x_3	$\sqrt{x_1^2+x_2^2+x_3^2}$	Disk plane (θ)	Airfoil (ϕ)
3a	16.3 (.414)	7.6 (.193)	9.0 (.229)	20.1 (.511)	-30°*	25°
3b	16.3 (.414)	7.6 (.193)	0.0	18.0 (.457)	0°	25°
3c	16.3 (.414)	7.6 (.193)	-9.0 (-.229)	20.1 (.511)	+30°**	25°
3d	0.0	18.0 (.457)	9.0 (.229)	20.1 (.511)	-30°	90°
3e	0.0	18.0 (.457)	0.0	18.0 (.457)	0°	90°
3f	0.0	18.0 (.457)	-9.0 (-.229)	20.1 (.511)	+30°	90°
4	-8.23 (-.209)	-35.7 (-.906)	18.3 (.465)	40.9 (1.04)	-30°	77°
5	-8.23 (-.209)	-35.7 (-.906)	0.0	36.6 (.931)	0	77°
6	-8.23 (-.209)	-35.7 (-.906)	-18.3 (-.465)	40.9 (1.04)	+30°	77°

* A minus sign indicates upstream of the propeller disk.
** A plus sign indicates downstream of the propeller disk.

Table 2.- Summary of Test Conditions for the Performance Measurement

Propeller		Inflow		
Type	$\beta_{.75}$	No Wake	With wake	
			t/c=1	t/c=3
Twin 1	16°	✓	✓	
"	20°	✓	✓	✓ *
"	24°	✓	✓	✓
"	28°	✓	✓	✓
"	32°	✓	✓	✓
"	36°	✓	✓	✓
"	40°	✓	✓	
Twin 3	15°	✓	✓	✓ *
"	16°	✓	✓	
"	20°	✓	✓	✓ *
"	24°	✓	✓	✓
"	28°	✓	✓	✓
"	32°	✓	✓	✓
"	36°	✓	✓	✓

*Noise measurements were made at these conditions.

Table 3.- Summary of Test Conditions for the Noise Measurement

Prop.	$\beta_{.75}$, deg	Airfoil angle, deg.	T_A, °F	ρ_A, slugs/ft^3	rpm	Thrust, lbf (N)	C_T	C_P	J	M_T
Twin 1	20	-	74.0	.0025	5250	40. (178.)	.089	.075	.614	.550
	20	15	75.0	.0025	5165	"	.092	.076	.626	.538
	20	20.4	74.8	.0025	5100	"	.095	.078	.636	.531
	20	-	74.0	.0025	6565	83. (369.)	.117	.091	.501	.680
	20	15.0	74.8	.0025	6485	"	.120	.092	.503	.670
	20	20.4	74.5	.0025	6469	"	.120	.093	.502	.670
Twin 3	20	-	77.0	.00247	5160	40. (178.)	.094	.081	.631	.536
	20	15.0	72.3	.0025	5080	" "	.096	.084	.642	.531
	20	20.4	73.2	.0025	5070	" "	.096	.081	.642	.529
	20	-	77.0	.00247	6510	83. (369.)	.119	.093	.502	.672
	20	15.0	72.7	.0025	6460	" "	.120	.094	.508	.670
	20	20.4	75.6	.00247	6460	" "	.122	.093	.506	.668
	15	-	74.7	.0025	7810	100. (445.)	.099	.067	.420	.805
	15	15.0	74.7	.00248	7789	"	.100	.067	.423	.803
	15	20.4	75.2	.00248	7768	"	.101	.066	.420	.800

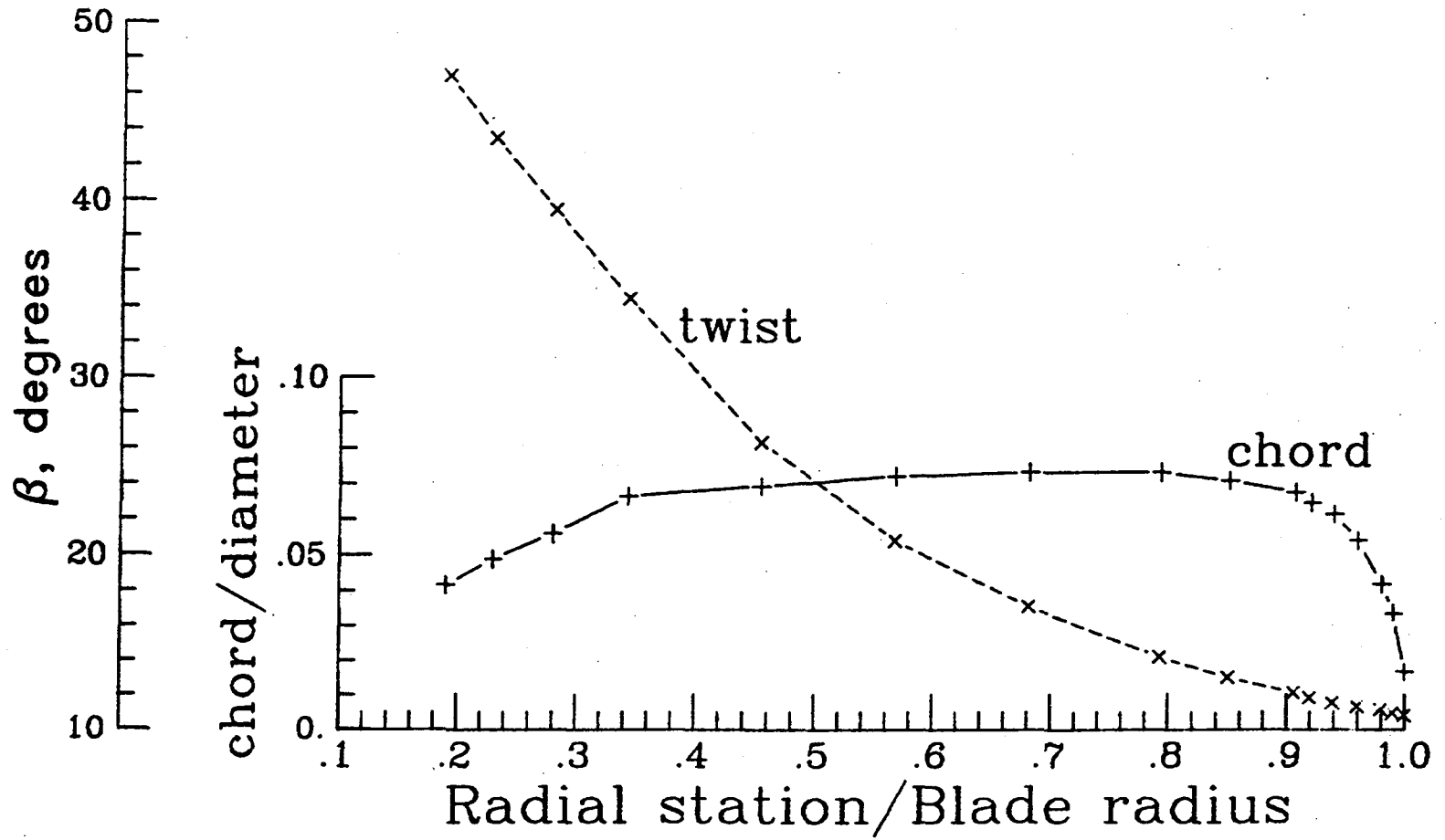

(a) Chord and twist distribution.

Figure 1.- Description of Twin 1 propeller.

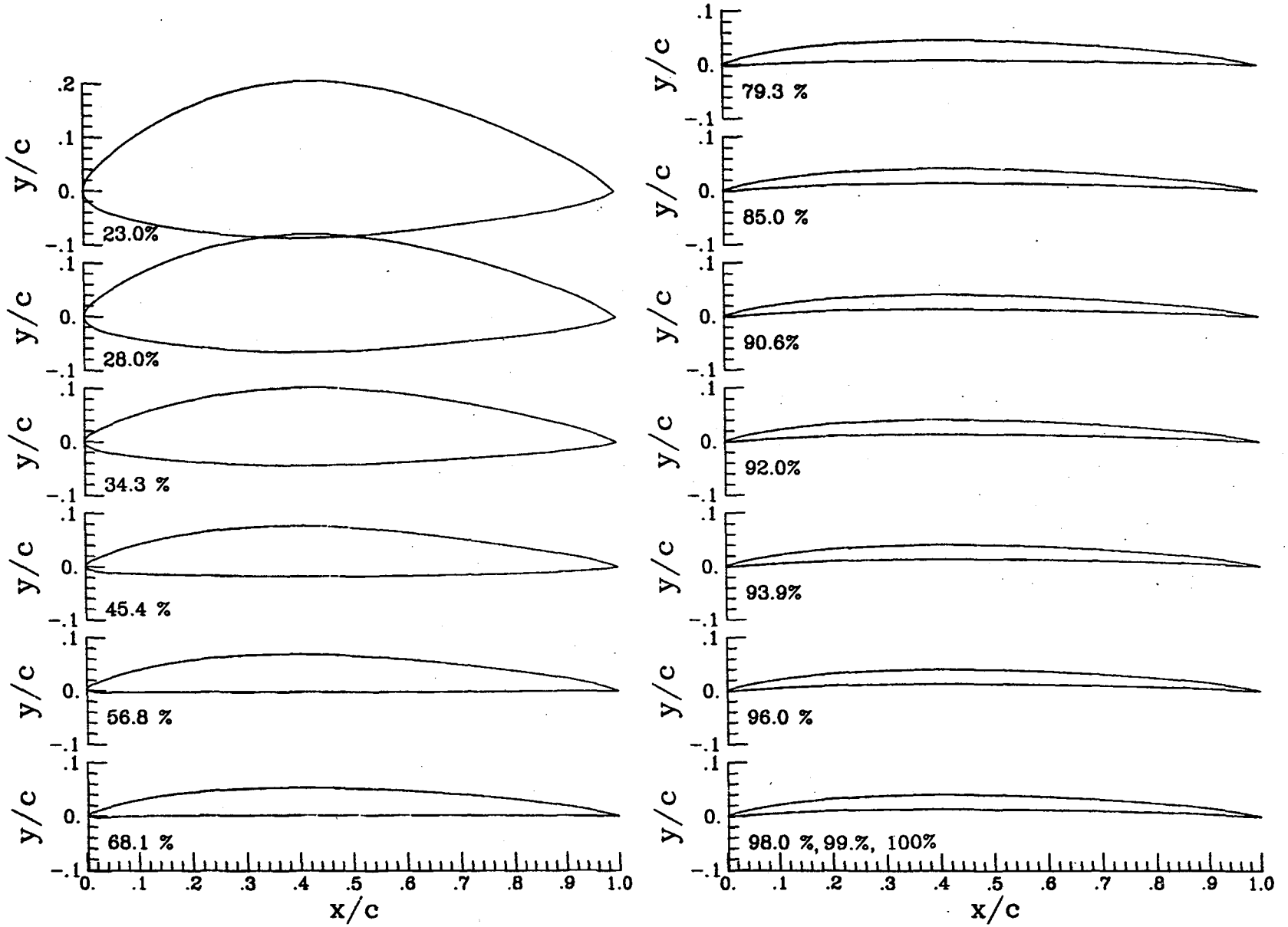

(b) Airfoil sections.

Figure 1.- Concluded.

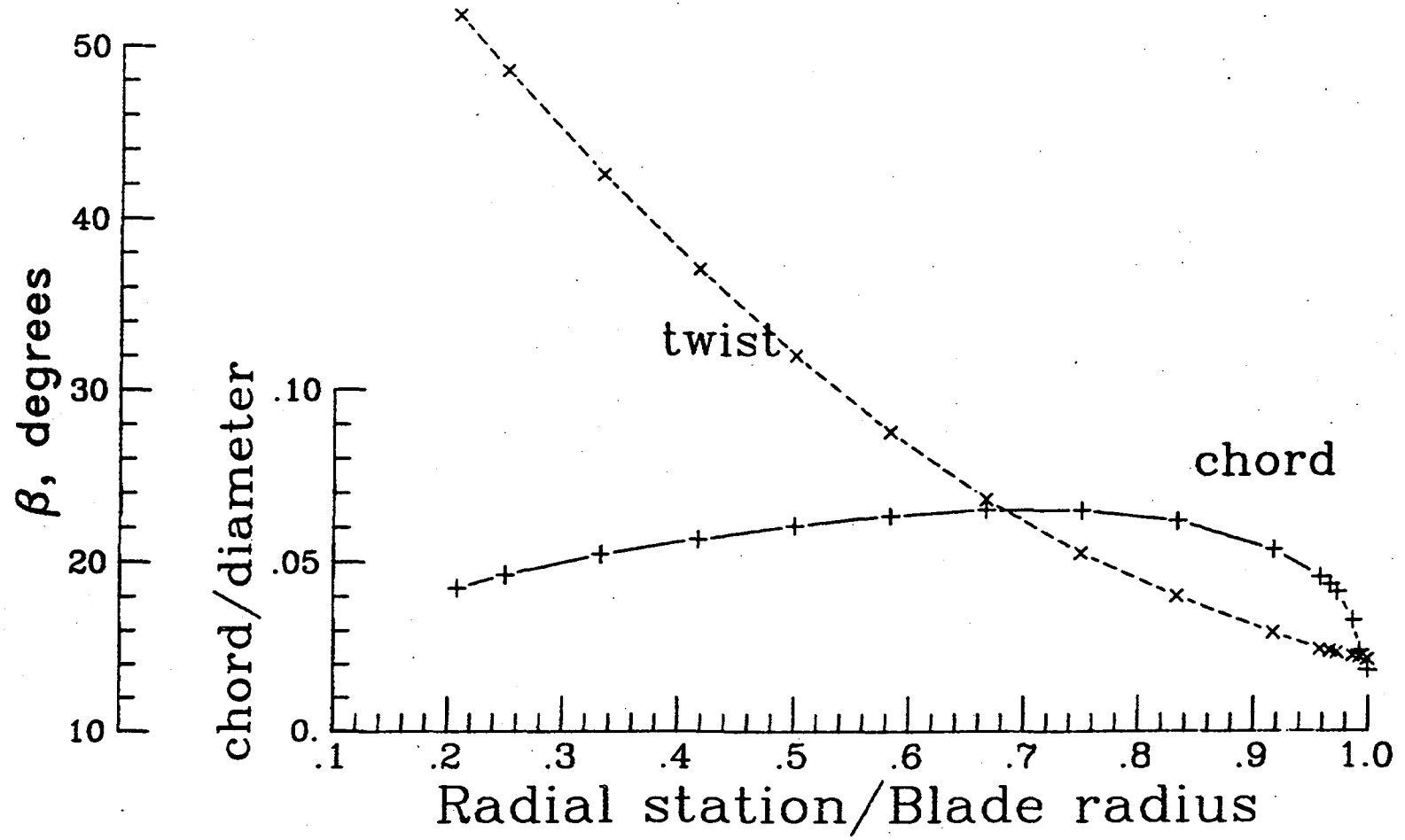

(a) Chord and twist distribution.

Figure 2.- Description of Twin 3 propeller.

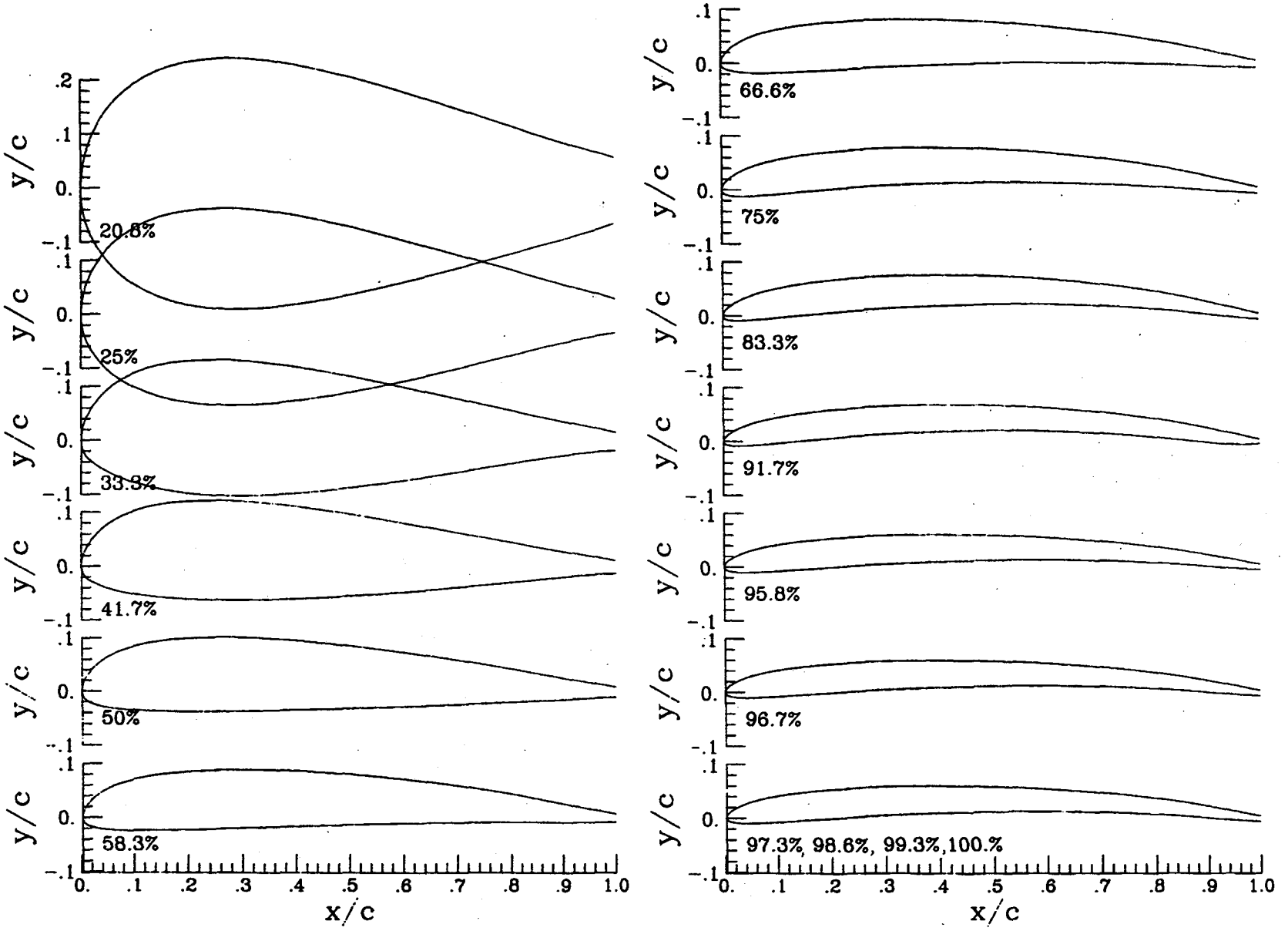

(b) Airfoil sections.

Figure 2.- Concluded.

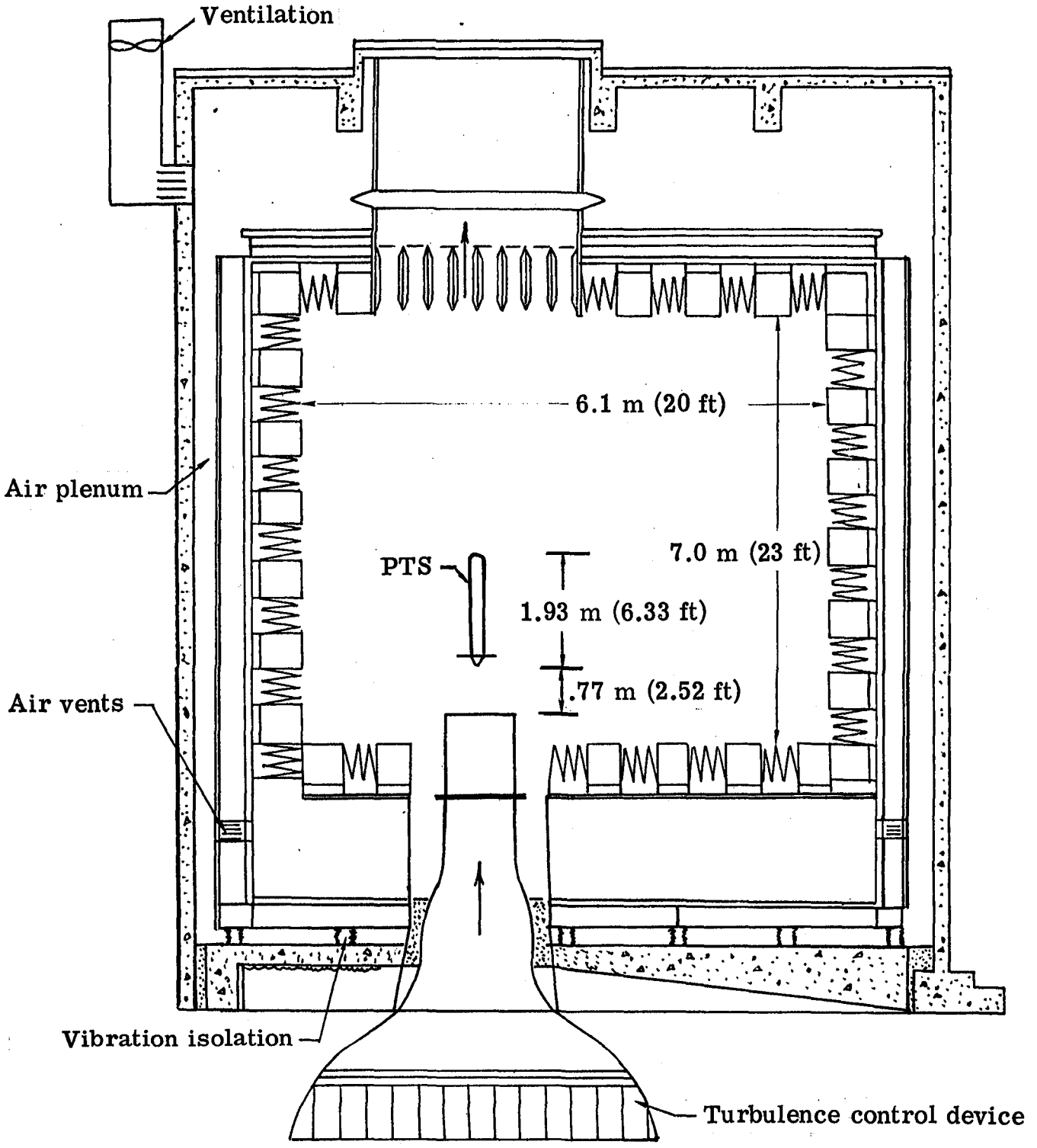

Figure 3.- Schematic of the PTS in the QFF.

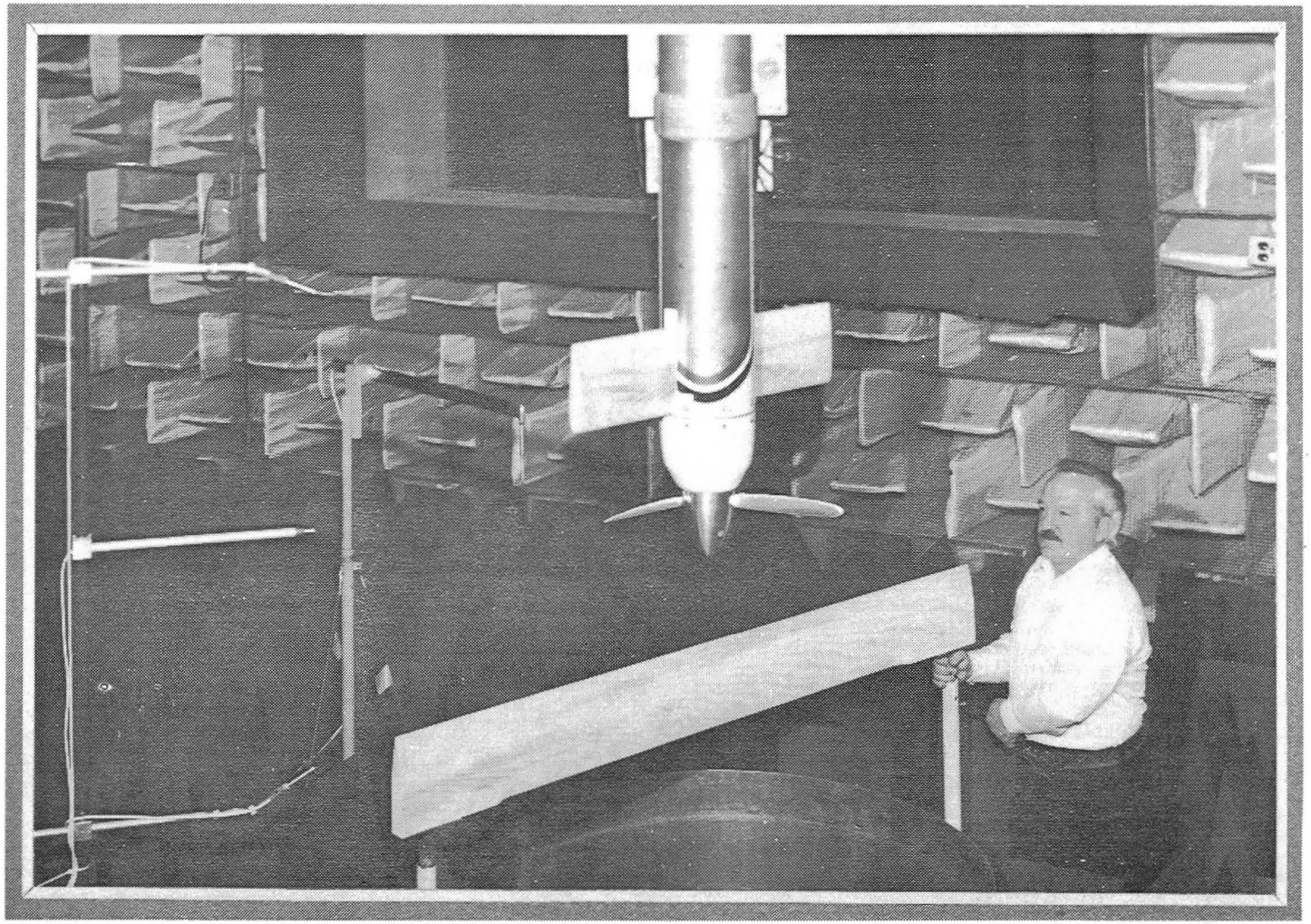

Figure 4.- Photo of the wake producing airfoil upstream of the propeller.

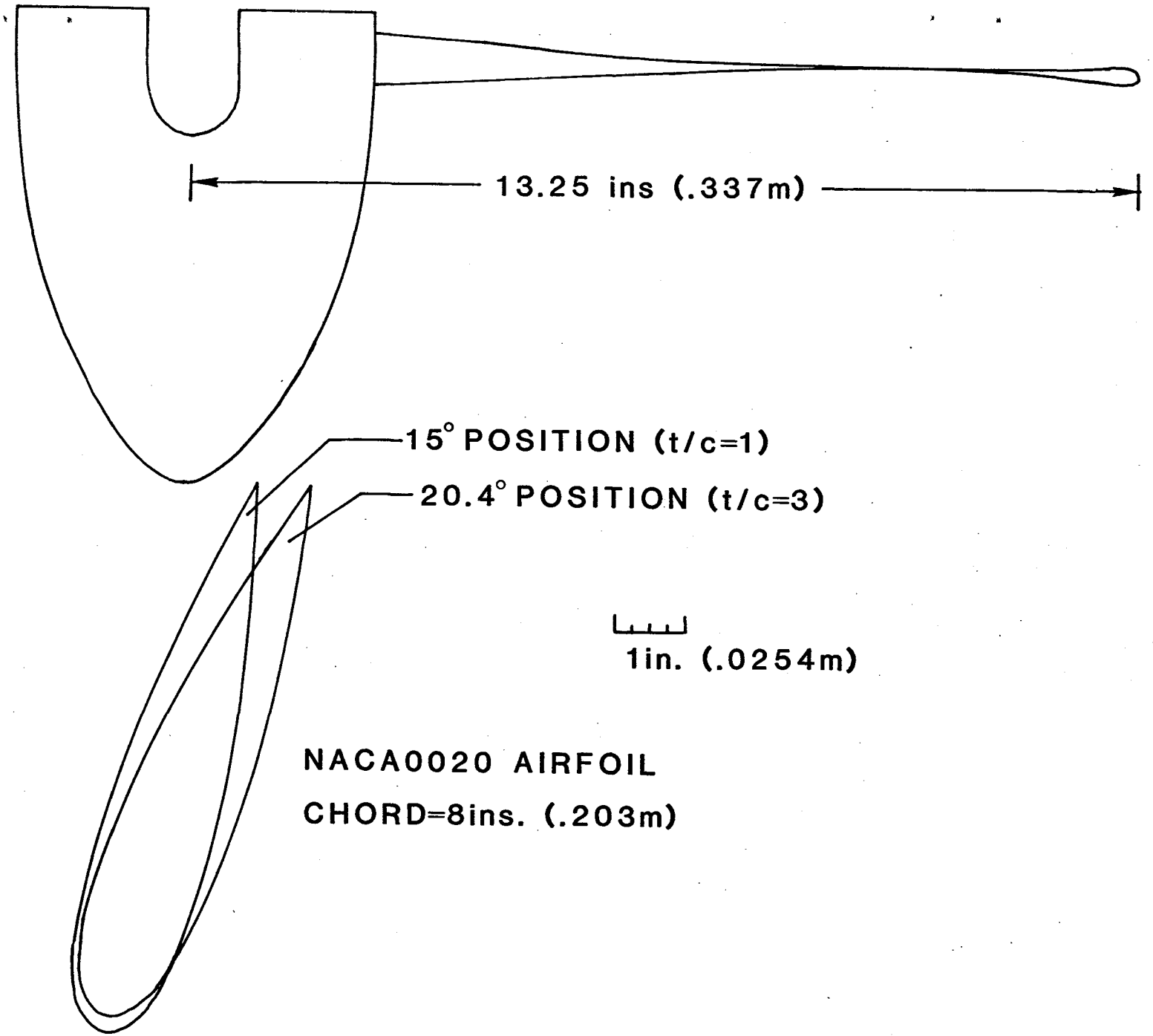

Figure 5.- Sketch giving positions and dimensions of the NACA 0020 airfoil used for producing the wake.

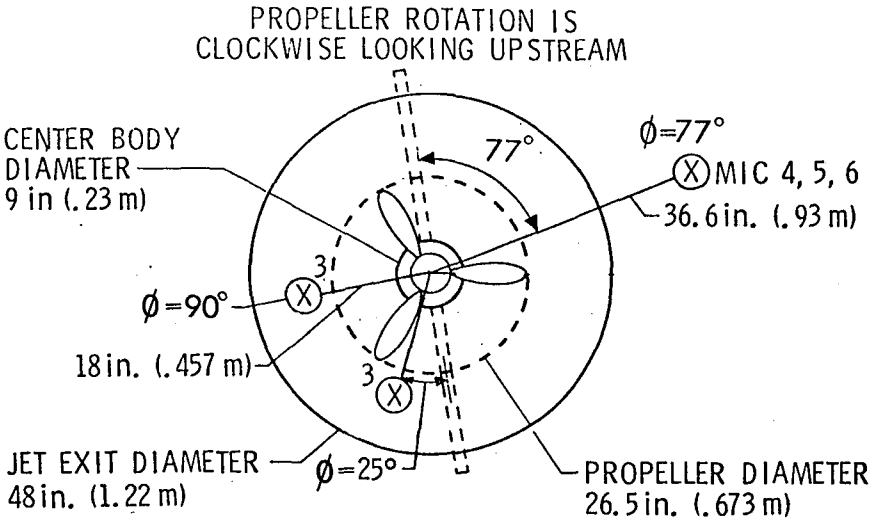

Plan view.

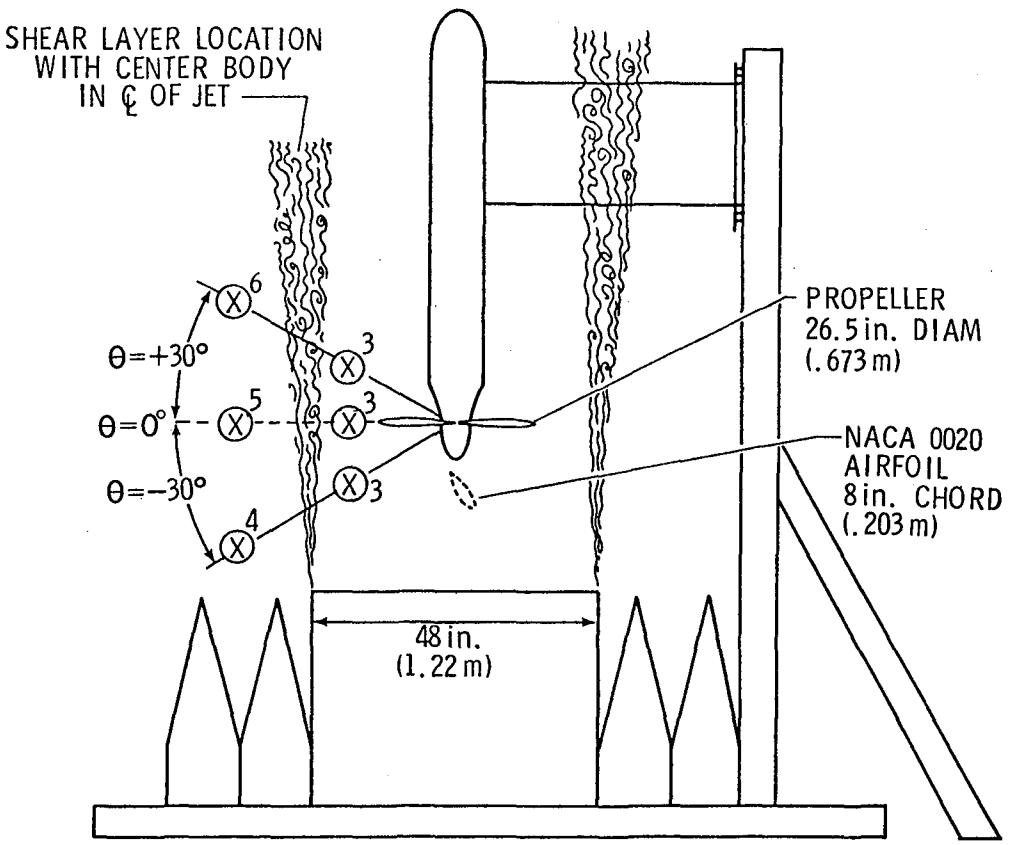

Side view.

Figure 6.- Schematic of the test setup.

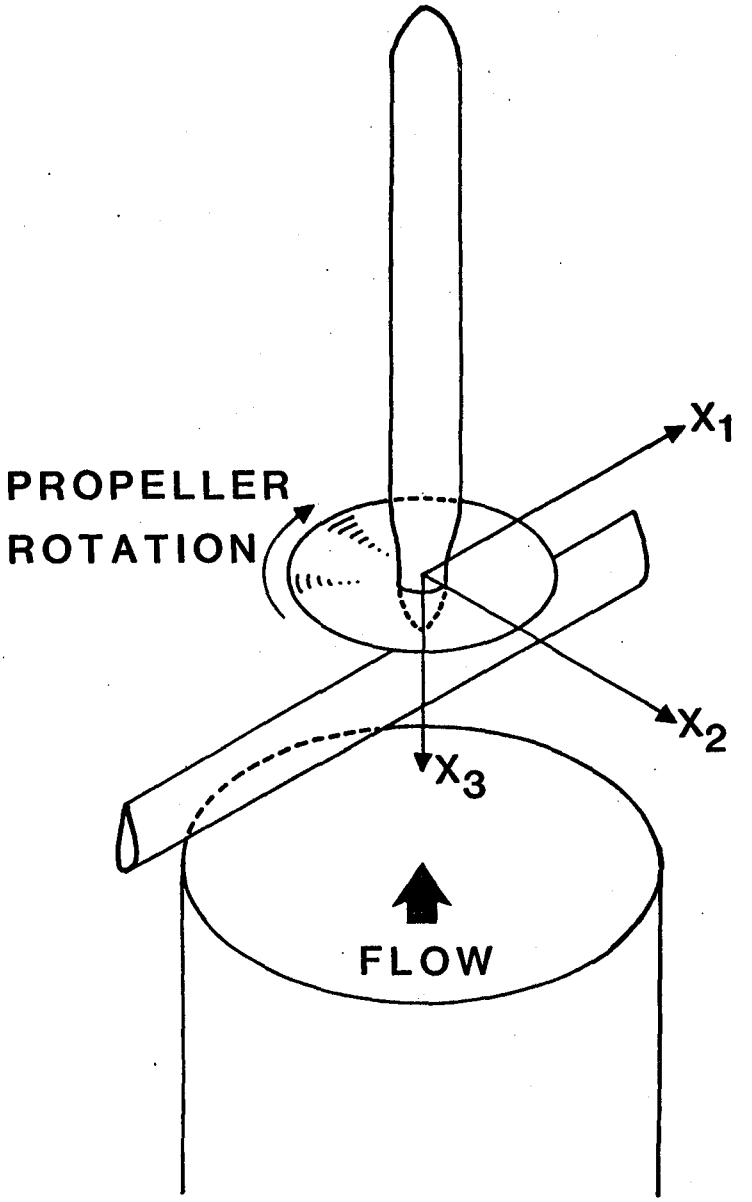

Figure 7.- Isometric drawing showing the coordinate system in which the microphone locations are defined.

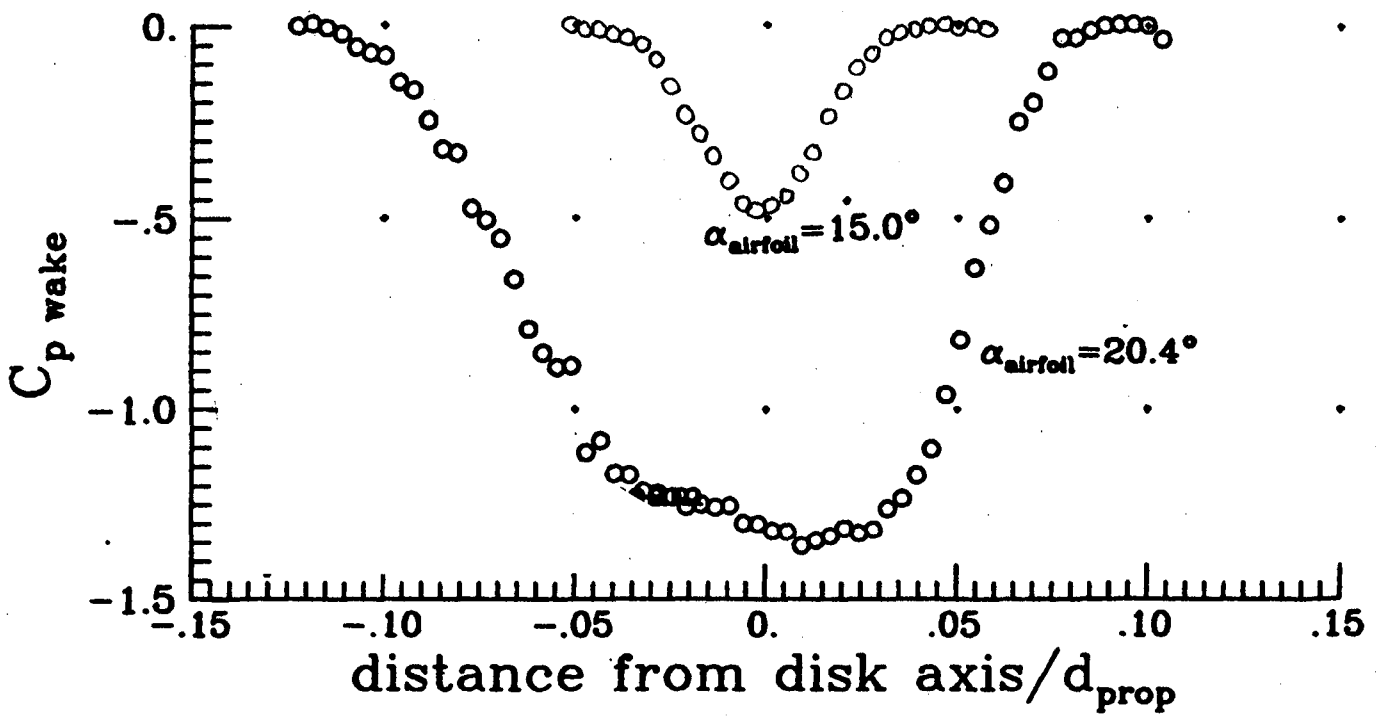

Figure 8.- Results from wake survey showing the velocity defect region produced by the airfoil. U_{jet} = 118.7 fps (36.2 m/s).

APPENDIX A

Performance Data

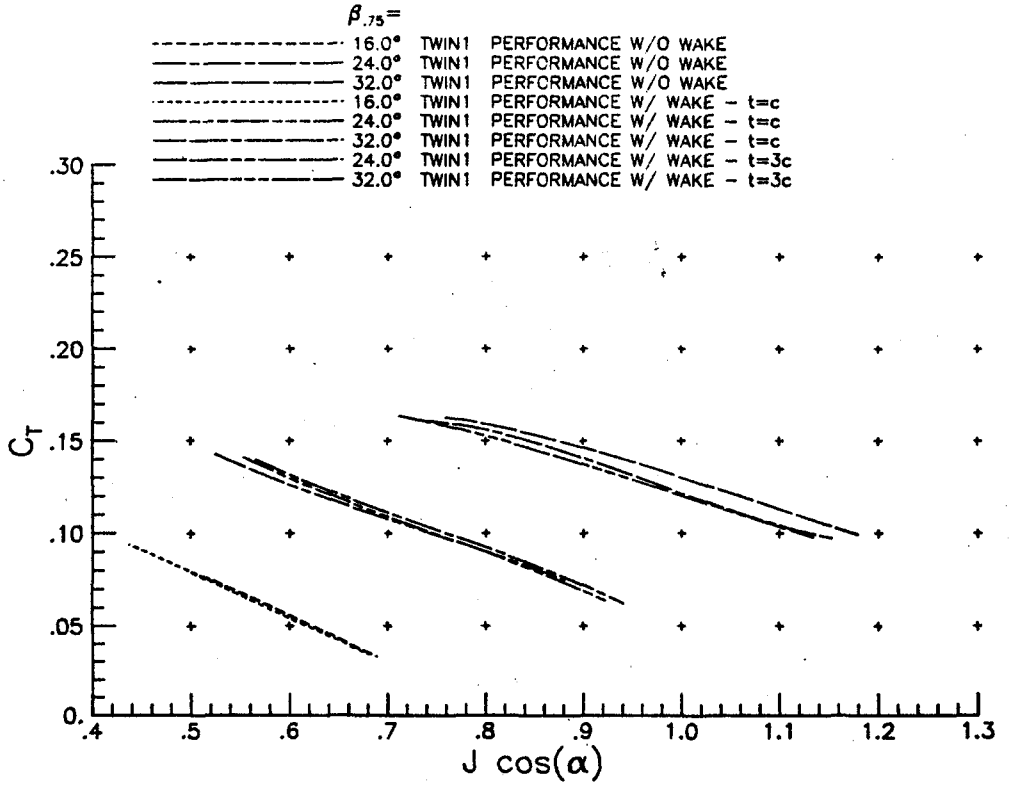

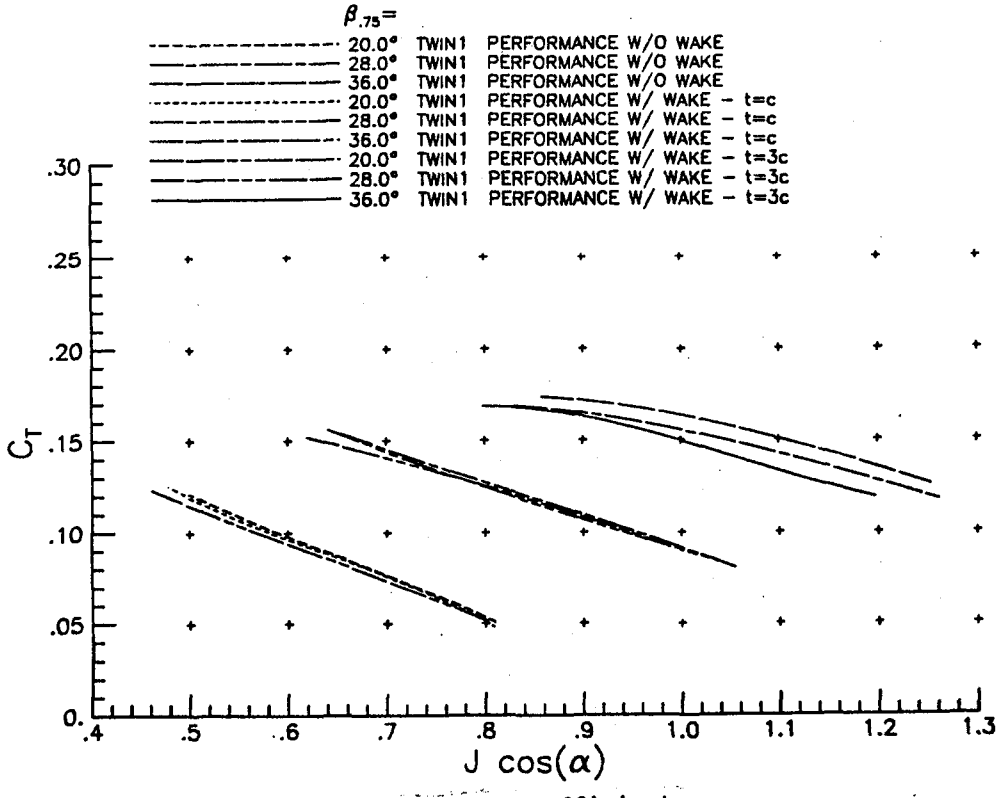

(a) Thrust coefficient.

Figure A1.- Propeller performance data for Twin 1

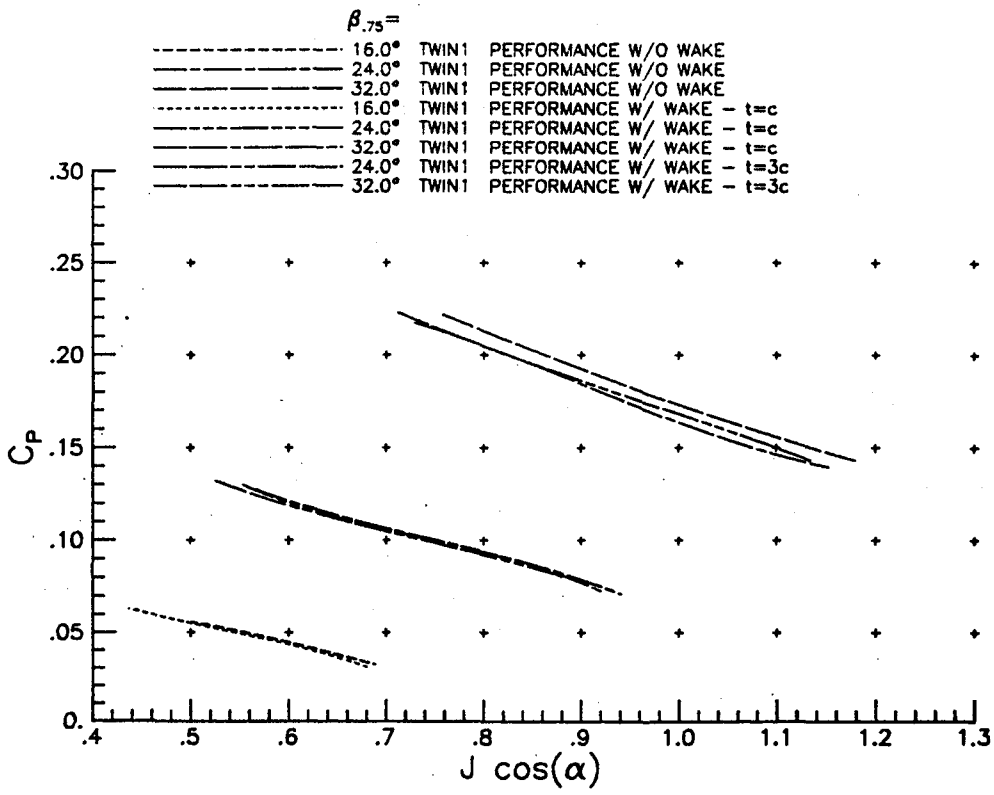

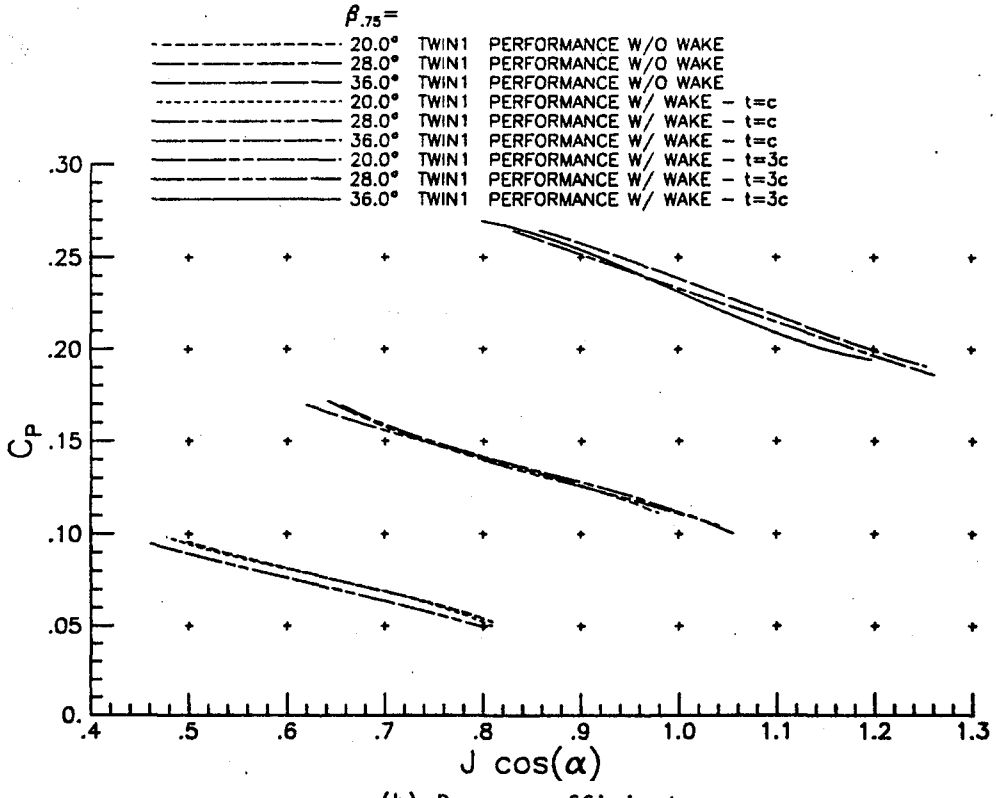

(b) Power coefficient.

Figure A1.- Continued.

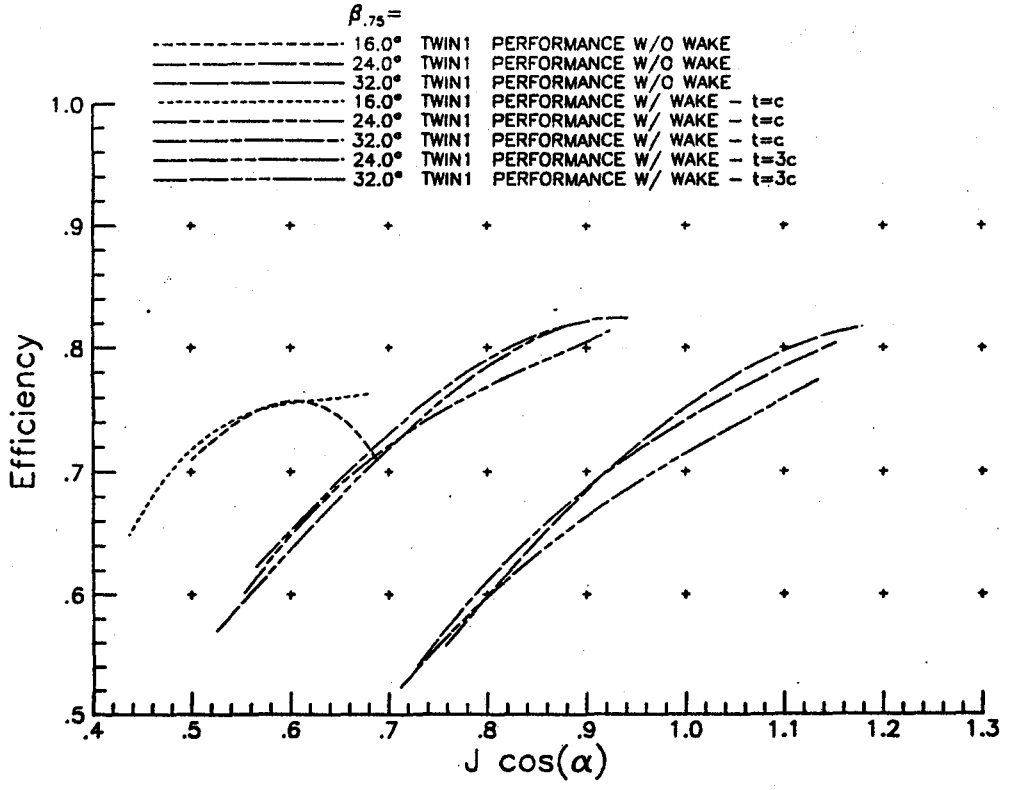

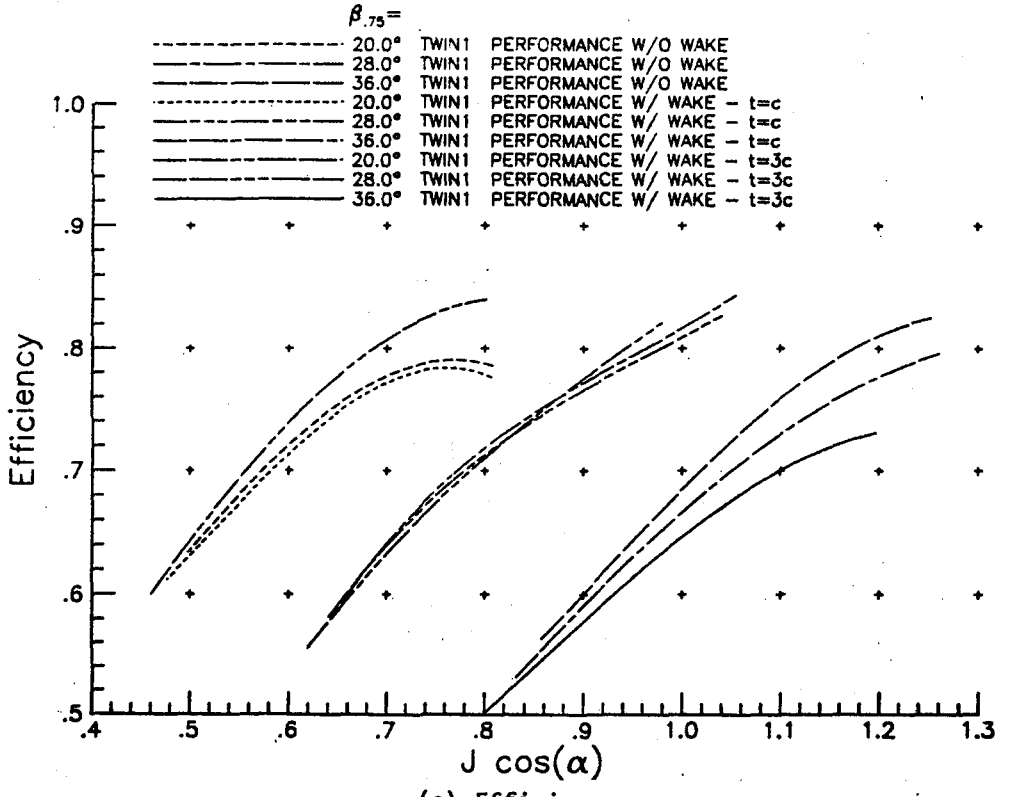

(c) Efficiency.

Figure A1.- Concluded.

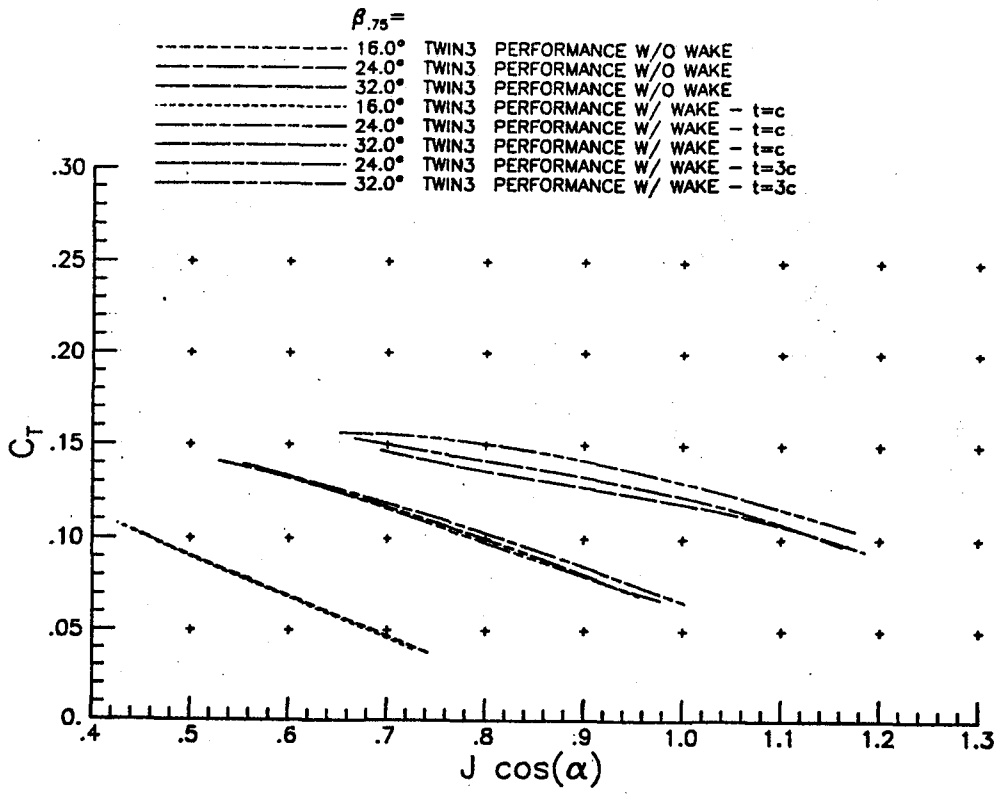

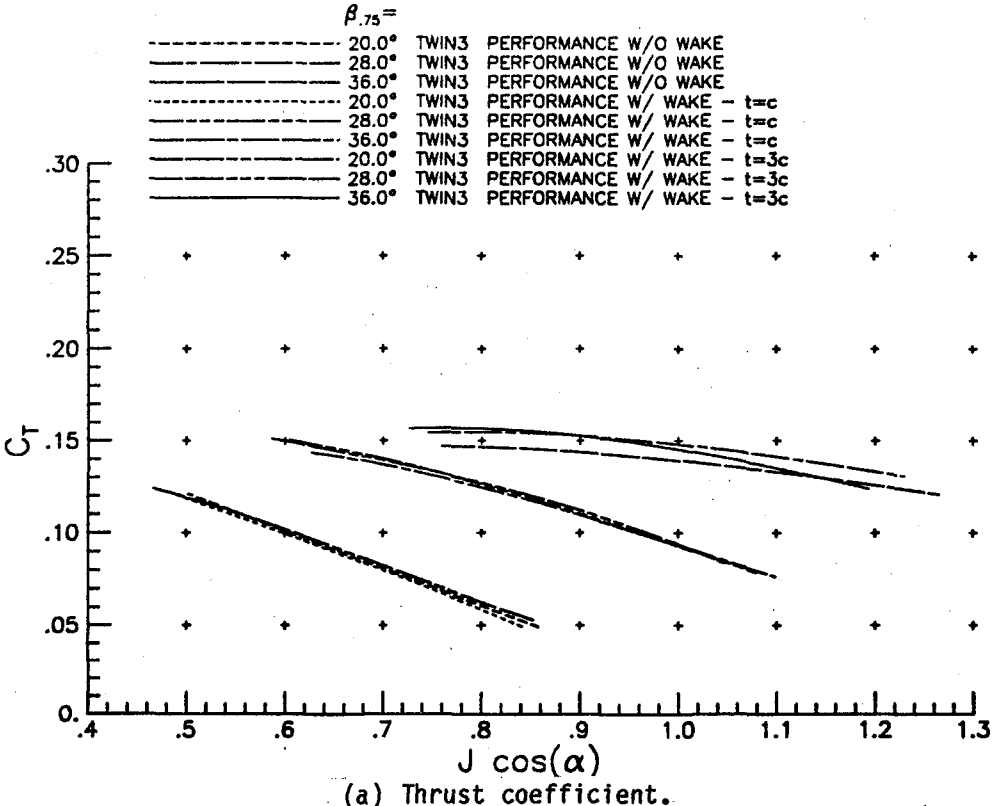

(a) Thrust coefficient.

Figure A2.- Propeller performance data for Twin 3.

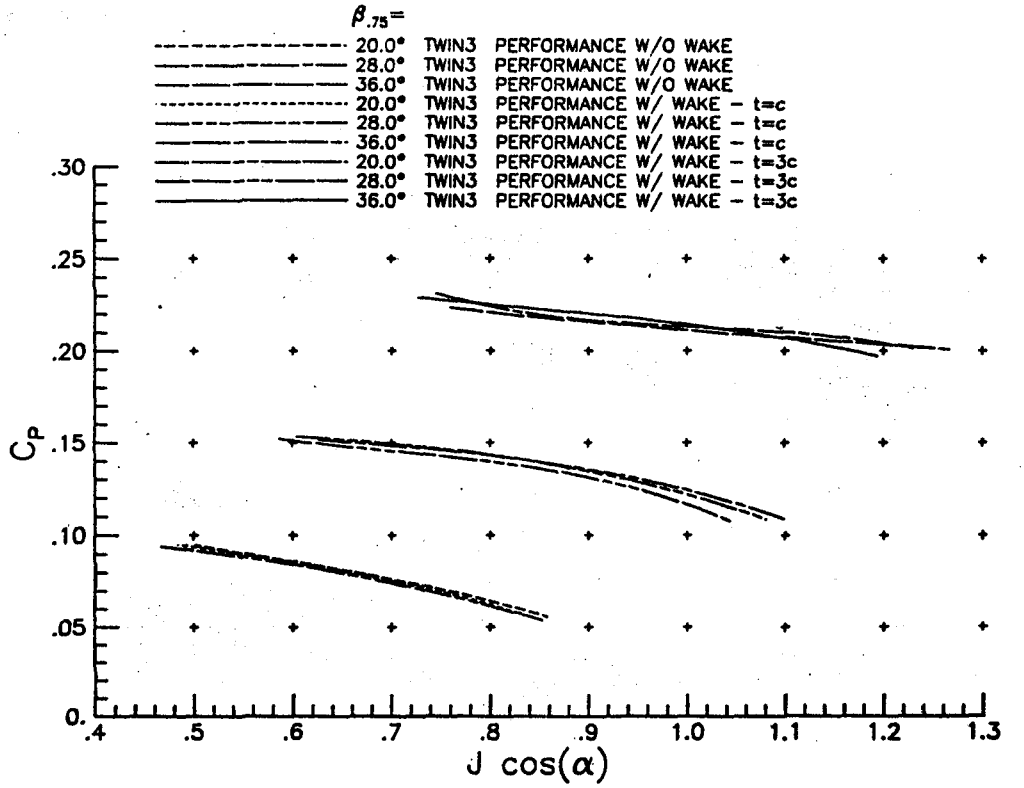

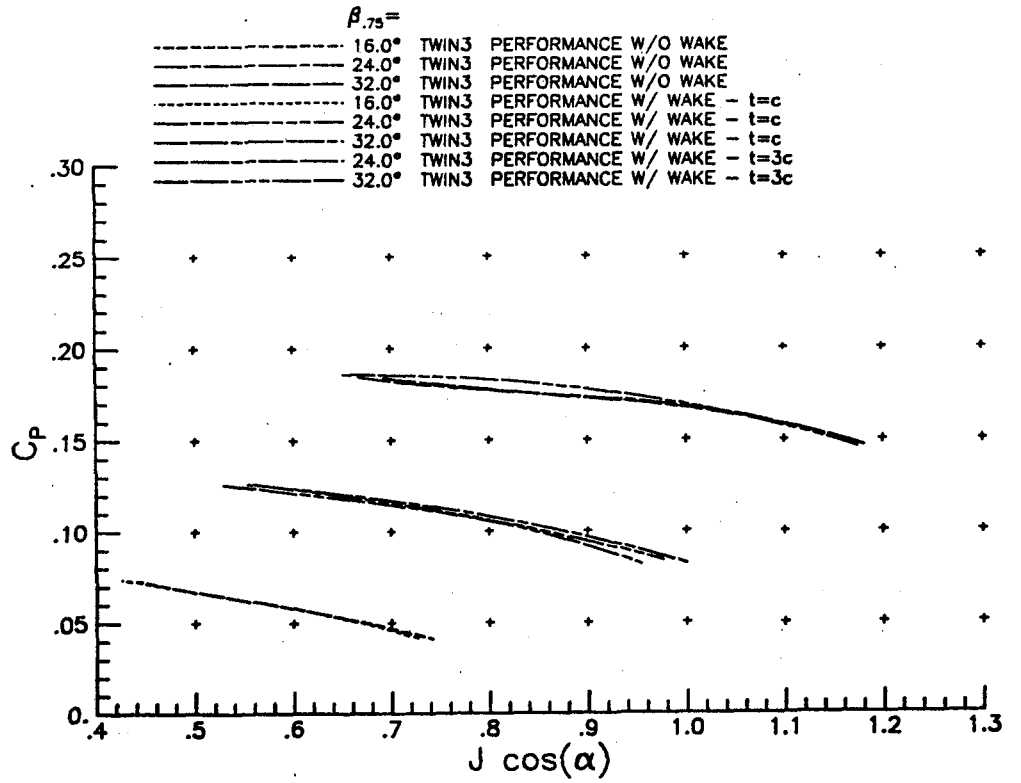

(b) Power coefficient.
Figure A2.- Continued.

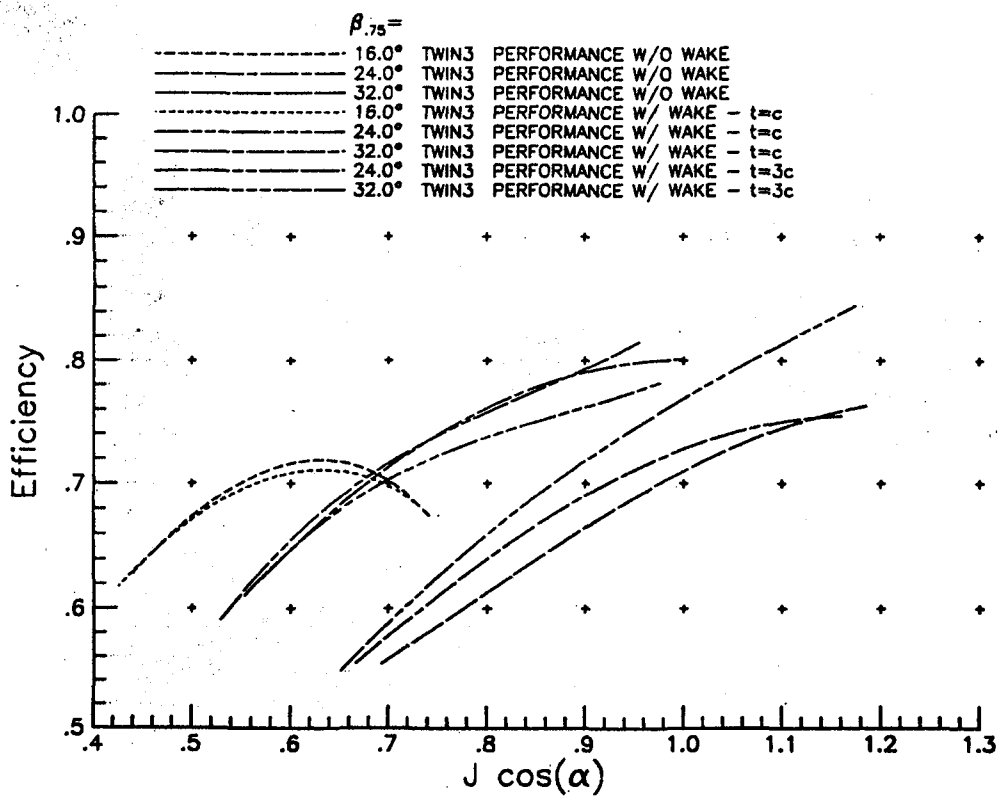

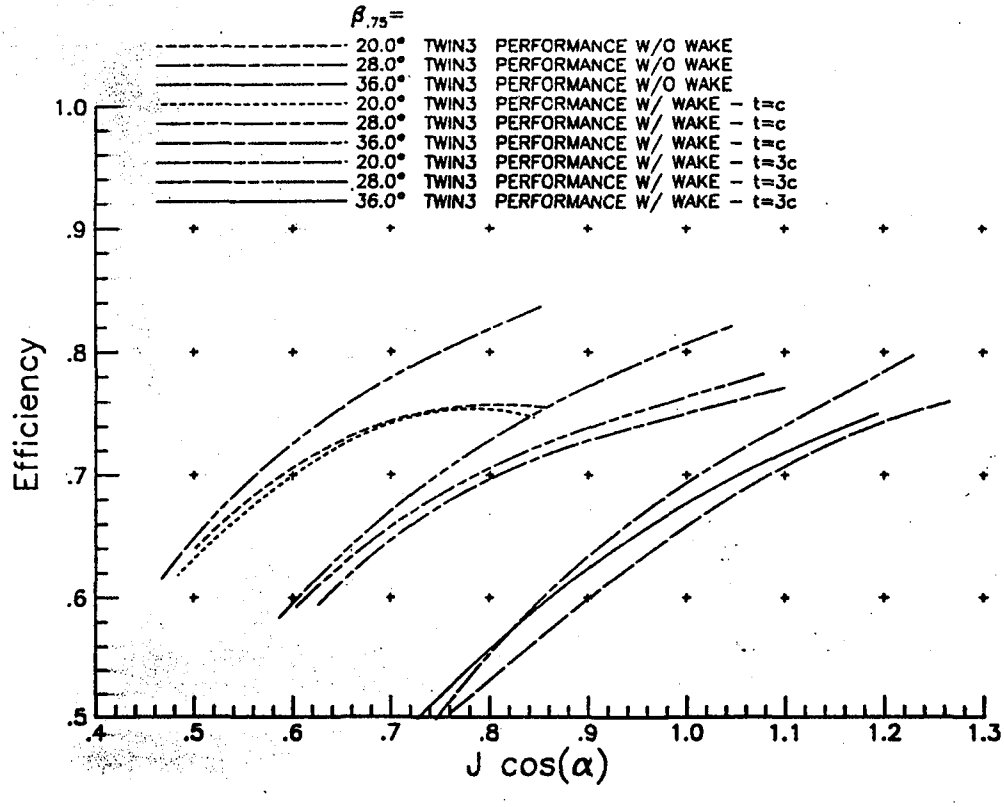

(c) Efficiency.

Figure A2.- Concluded.

APPENDIX B

Noise Data

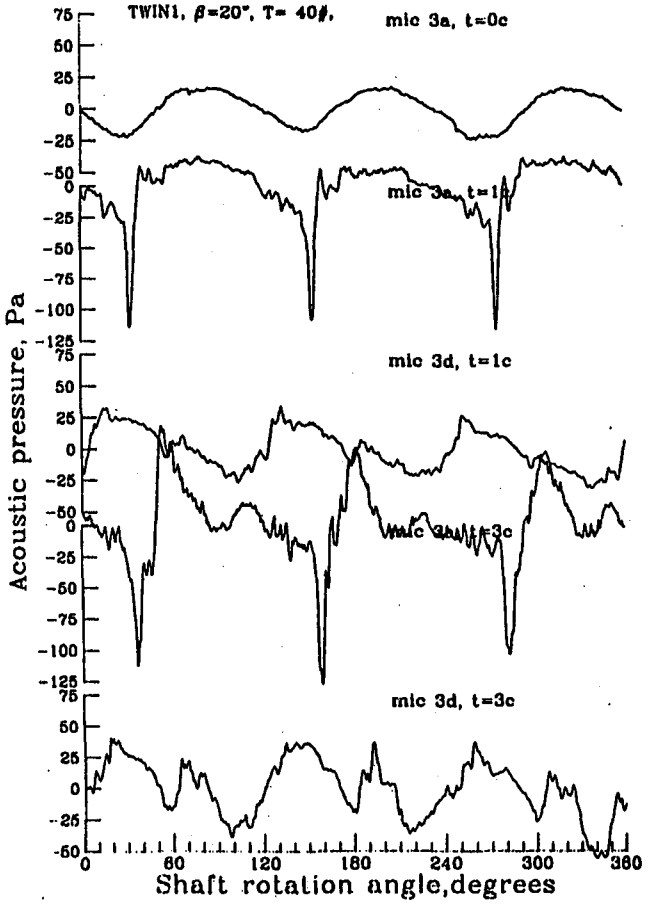

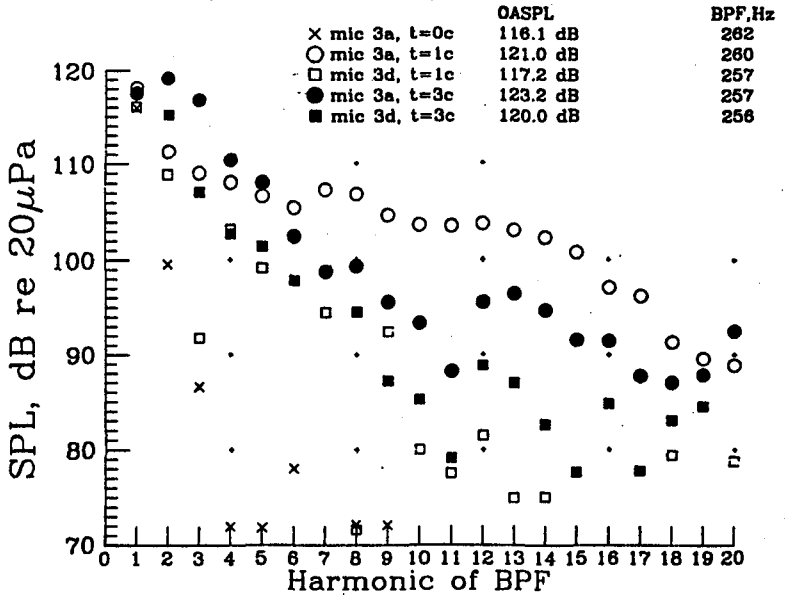

(a) 30° upstream (θ = -30°), microphone 3.

Figure B1.- Noise data for Twin 1, $\beta_{.75}$ = 20°, 40 lbf of thrust.

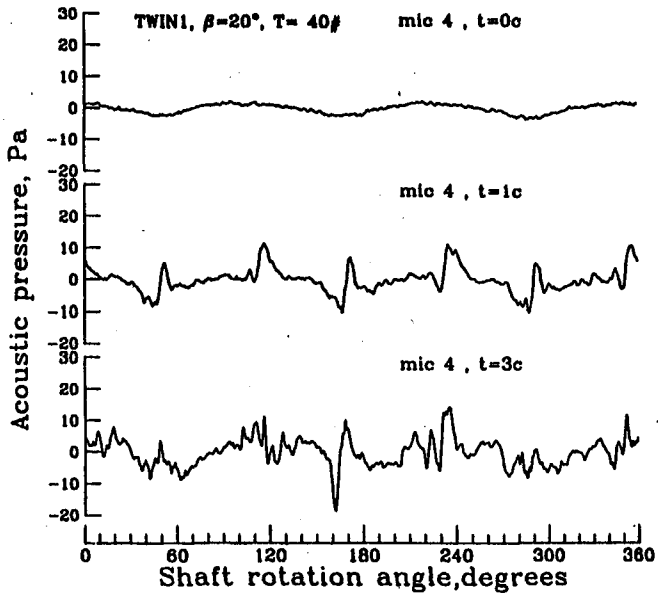

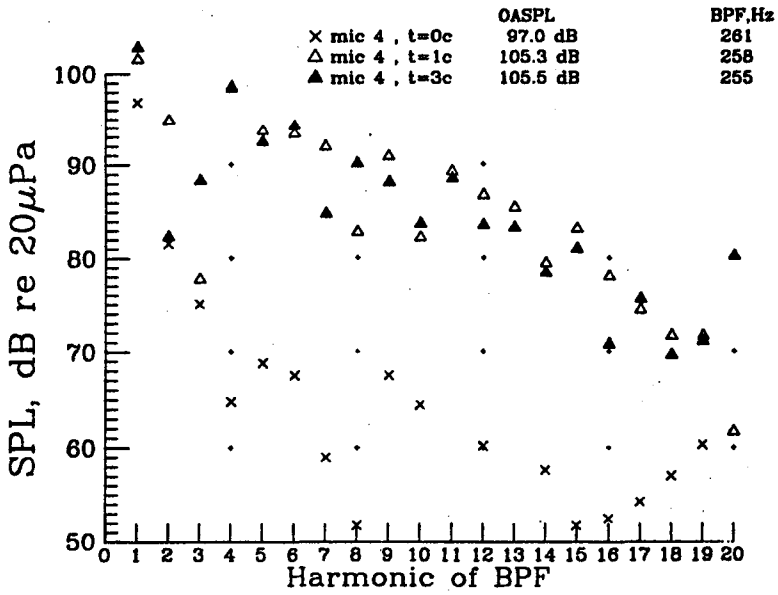

(b) 30° upstream (θ = -30°), microphone 4.

Figure B1.- Continued.

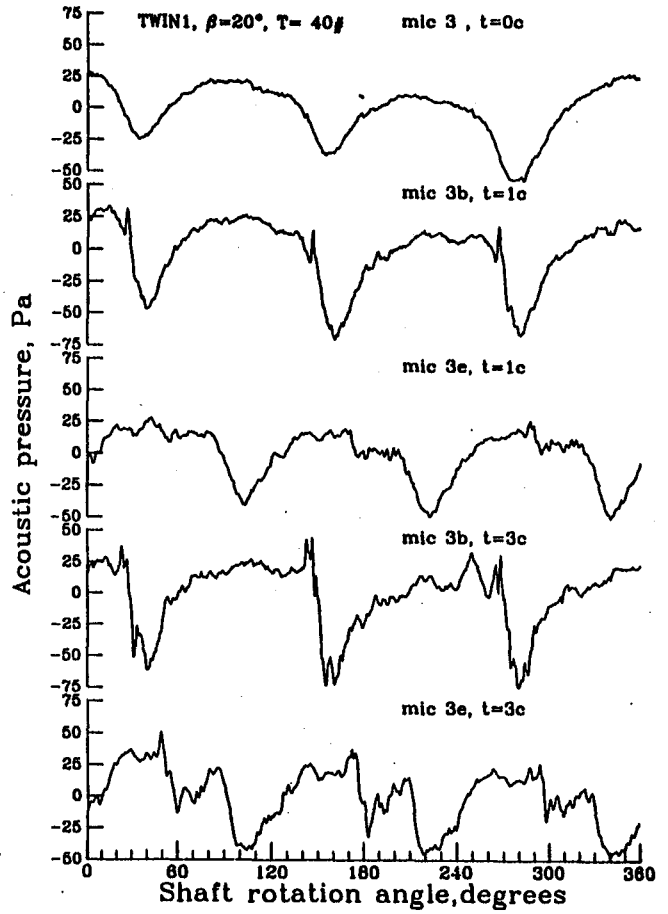

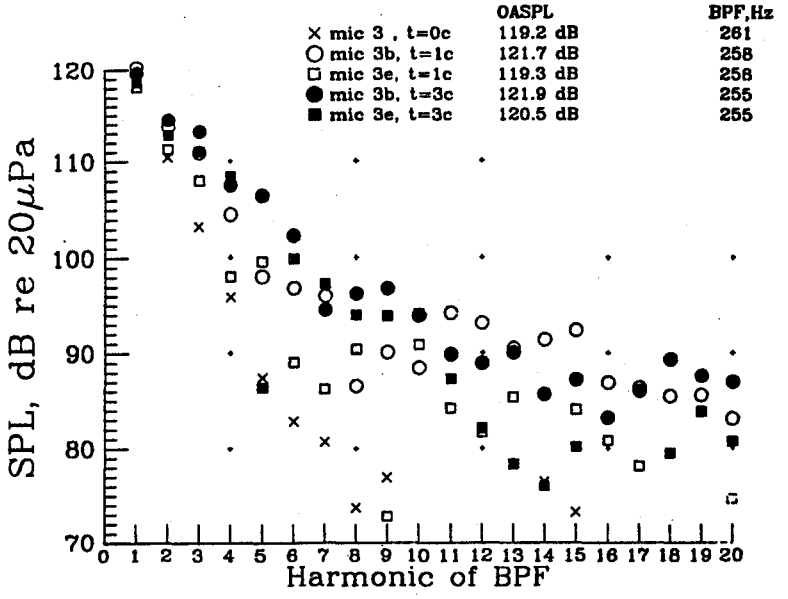

(c) inplane (θ = 0°), microphone 3.

Figure B1.- Continued.

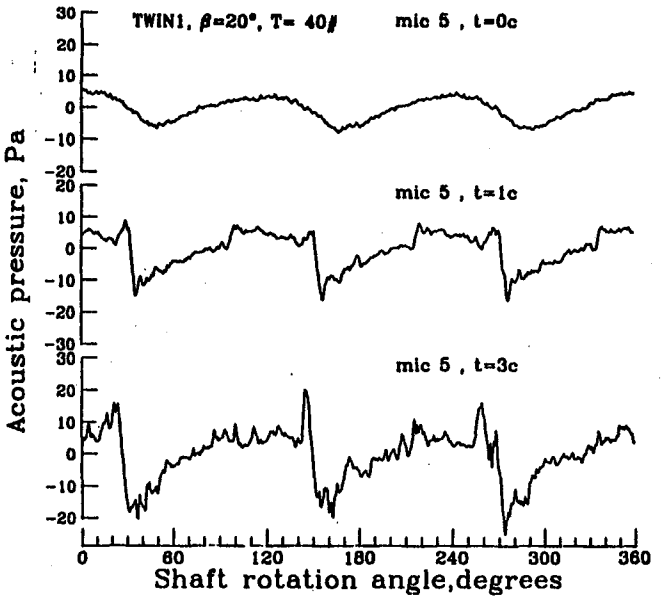

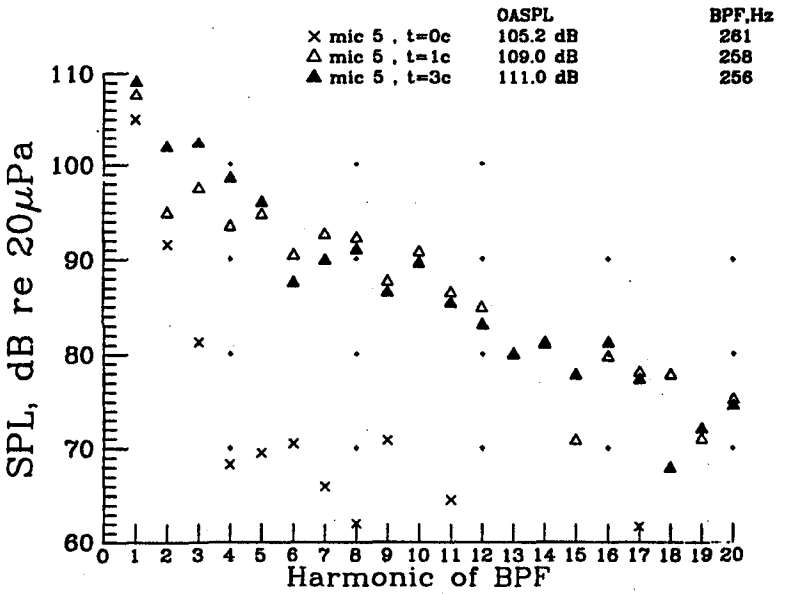

(d) inplane (θ = 0°), microphone 5.

Figure B1.- Continued.

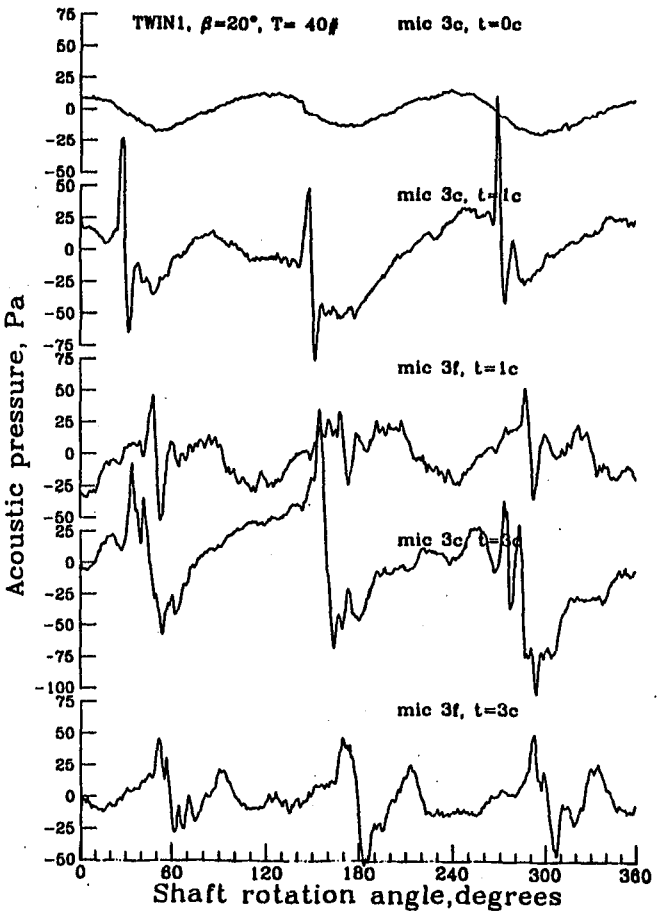

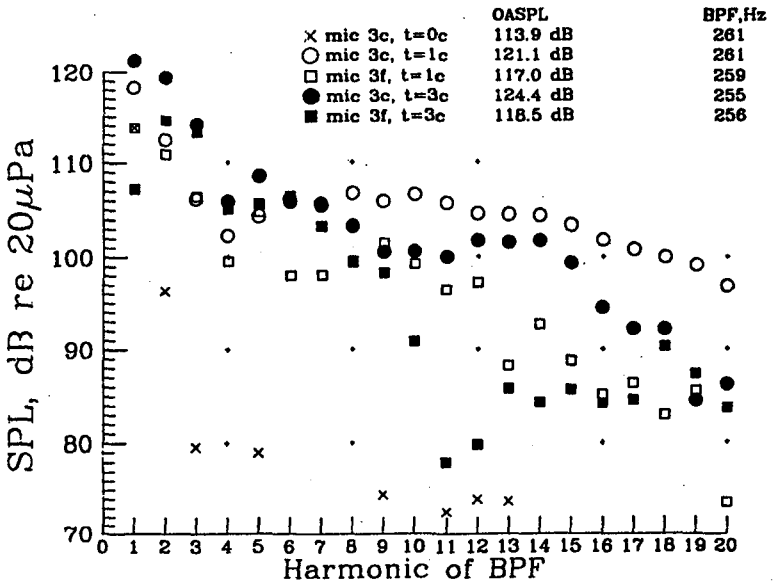

(e) 30° downstream (θ = 30°), microphone 3.

Figure B1.- Continued.

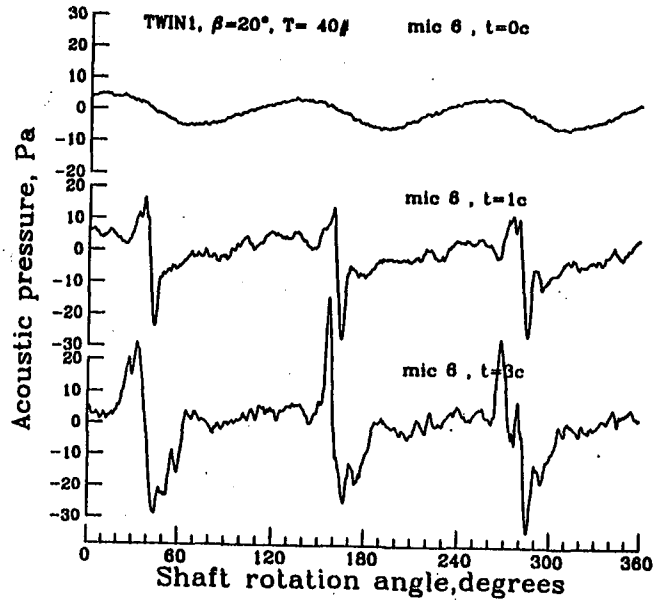

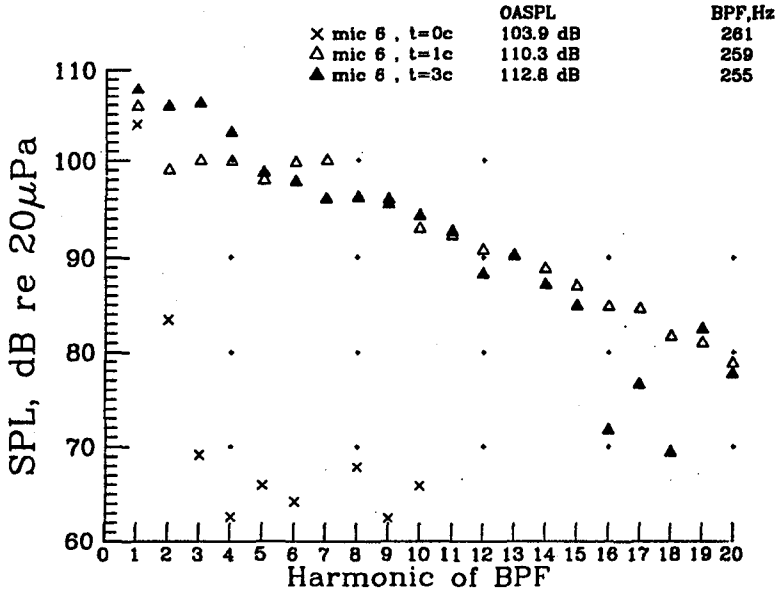

(f) 30° downstream (θ = 30°), microphone 6.

Figure B1.- Concluded.

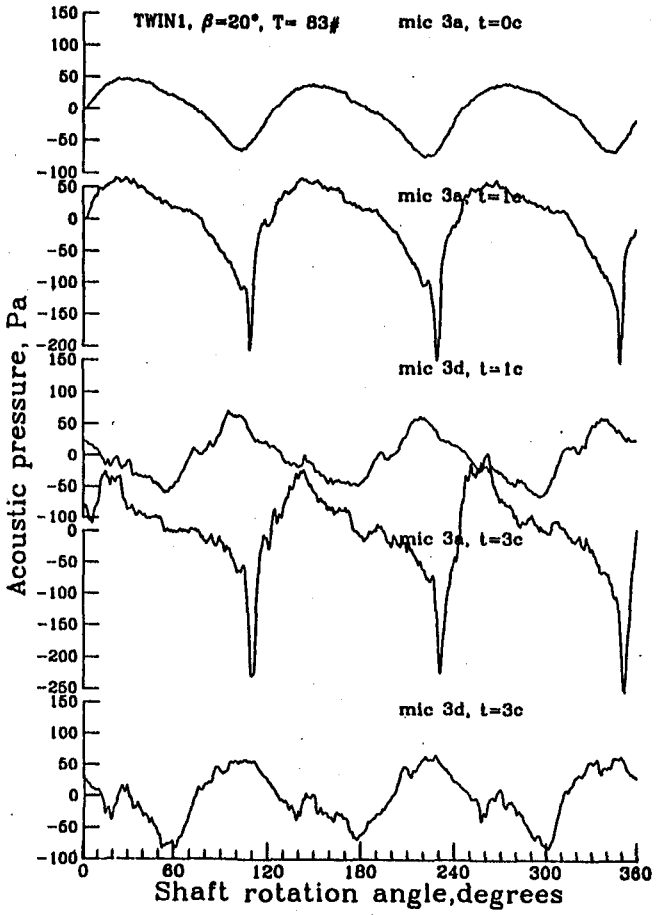

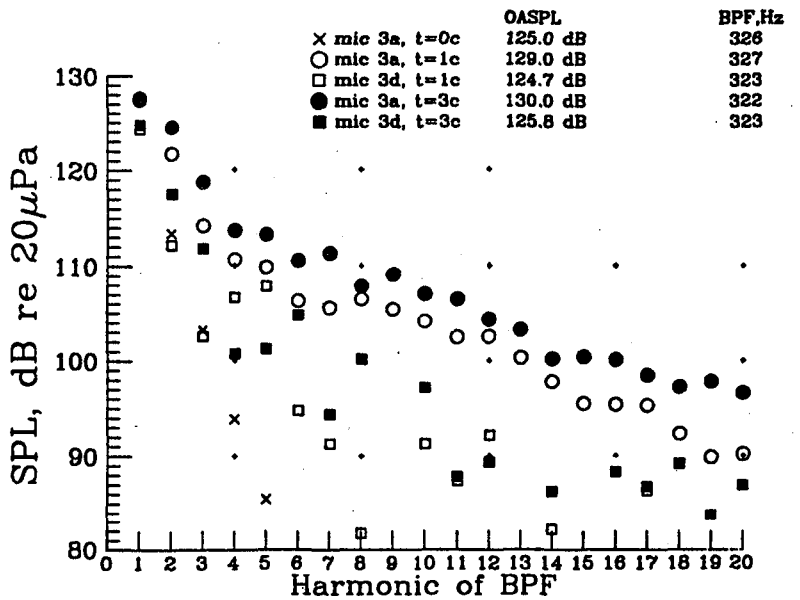

(a) 30° upstream (θ = -30°), microphone 3.

Figure B2.- Noise data for Twin 1, $\beta_{.75}$ = 20°, 83 lbf of thrust.

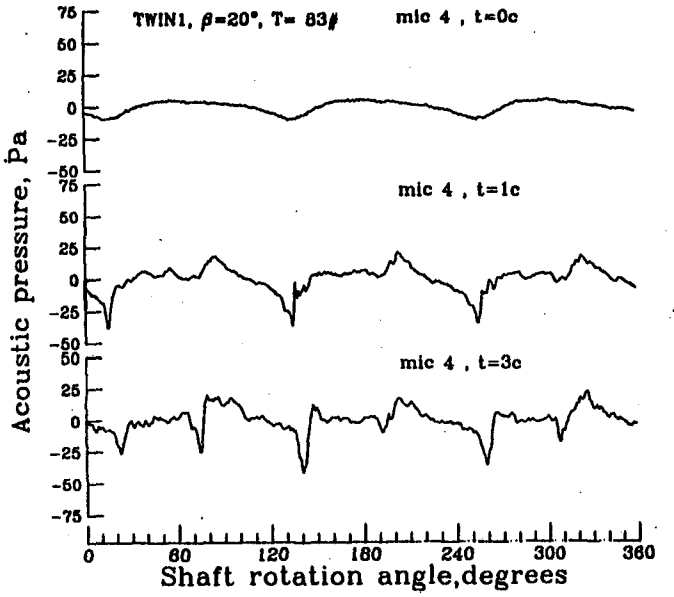

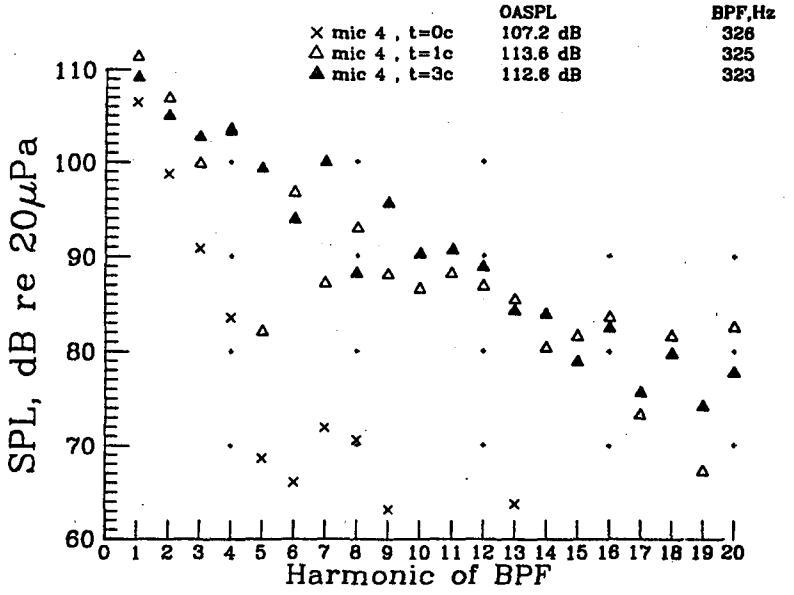

(b) 30° upstream (θ = -30°), microphone 4.

Figure B2.- Continued.

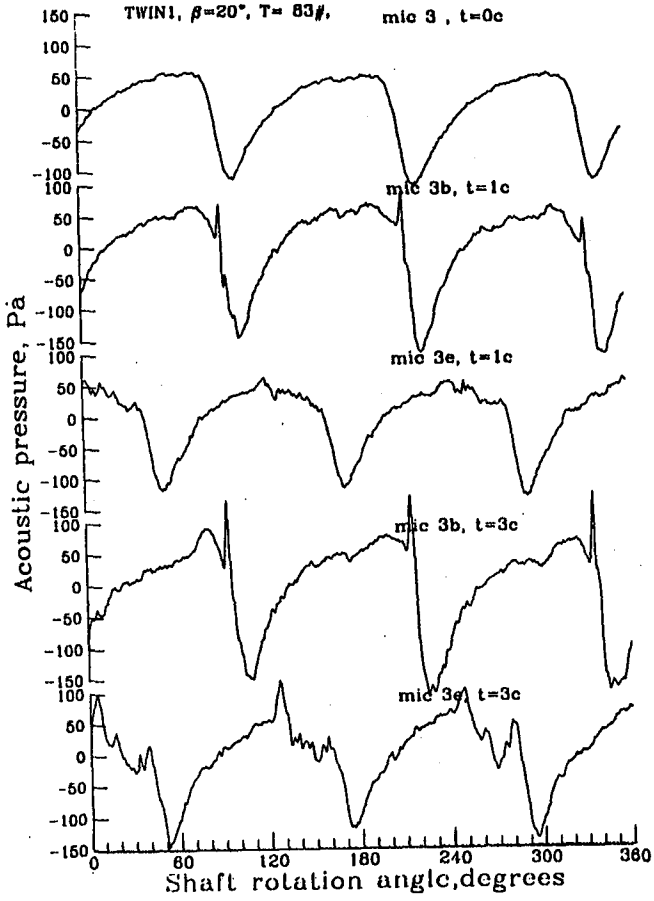

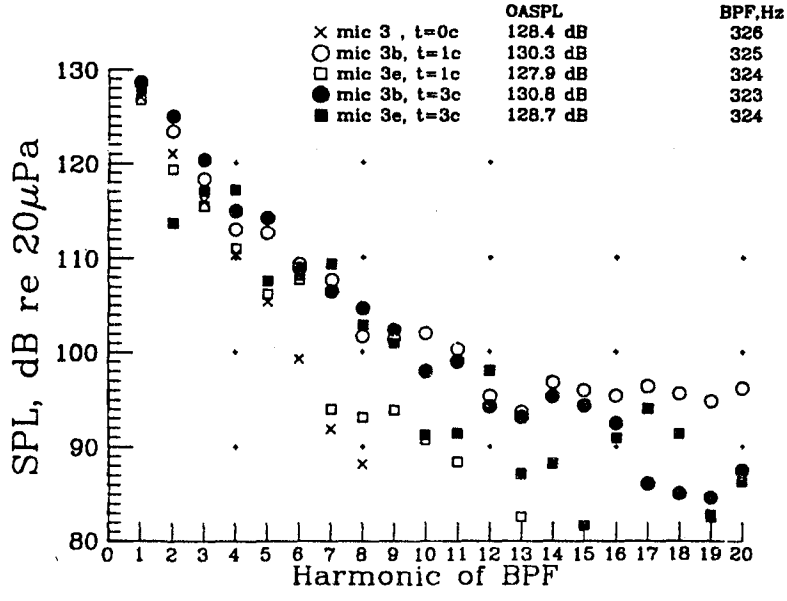

(c) inplane (θ = 0°), microphone 3.

Figure B2.- Continued.

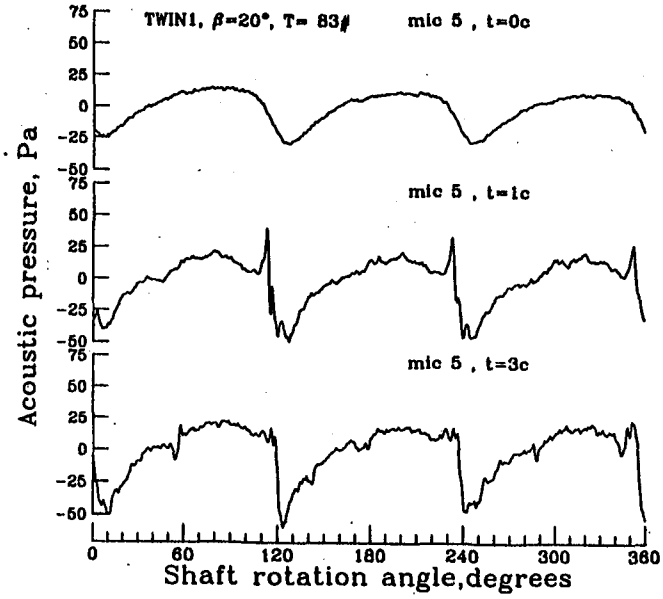

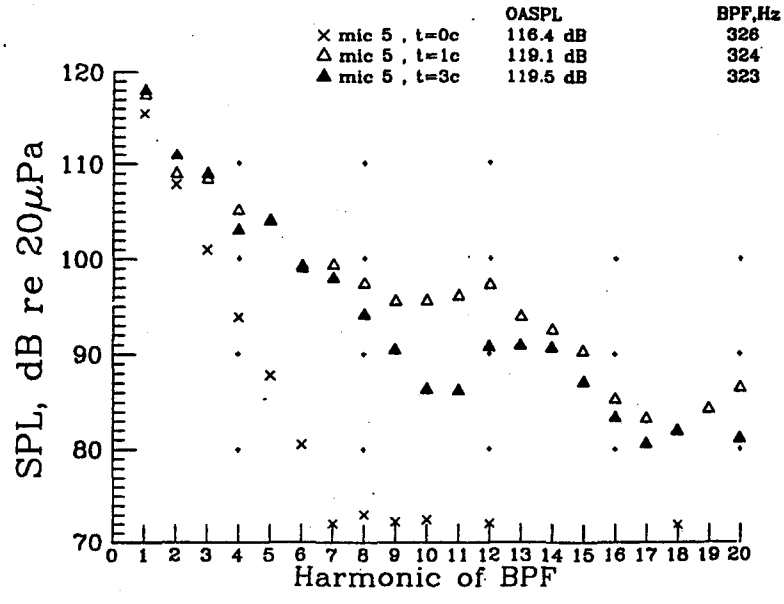

(d) inplane (θ = 0°), microphone 5.

Figure B2.- Continued.

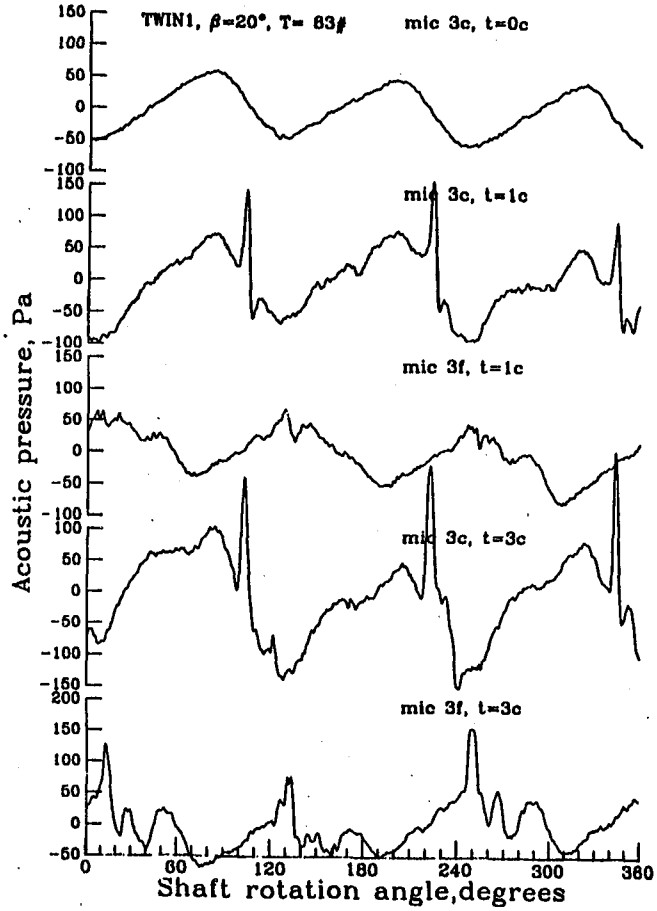

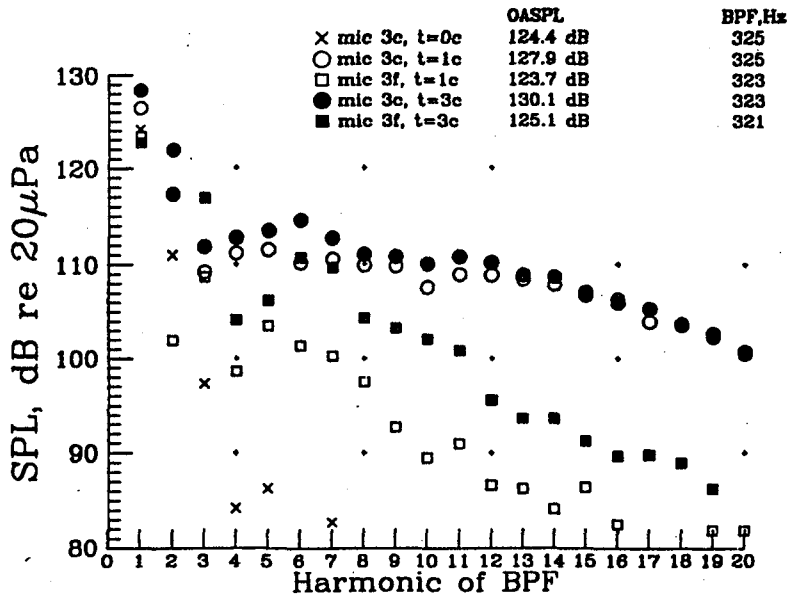

(e) 30° downstream (θ = 30°), microphone 3.

Figure B2.- Continued.

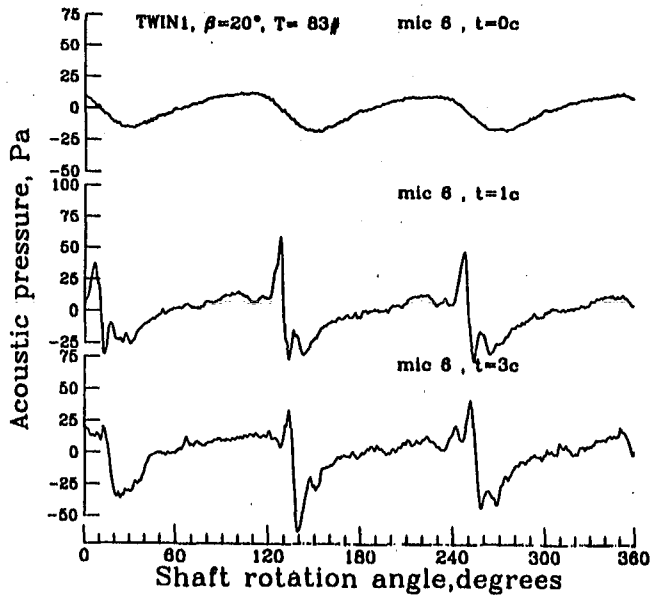

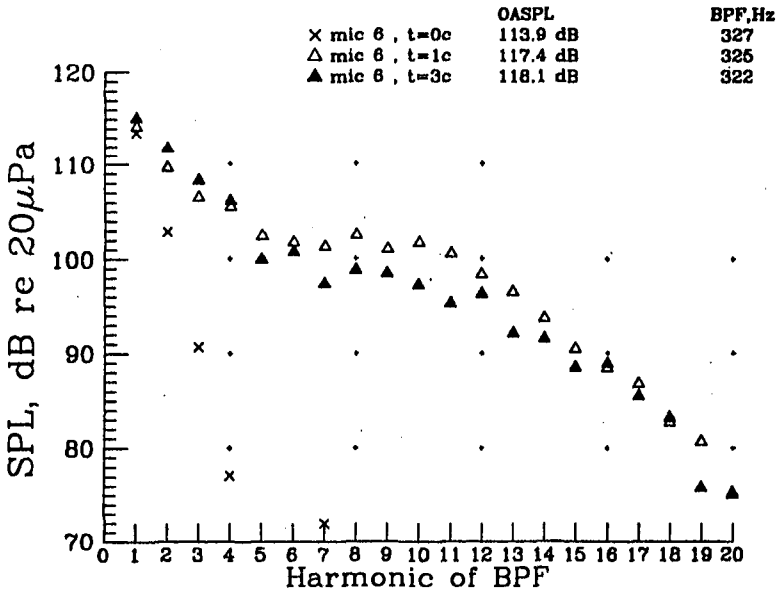

(f) 30° downstream (θ = 30°), microphone 6.

Figure B2.- Concluded.

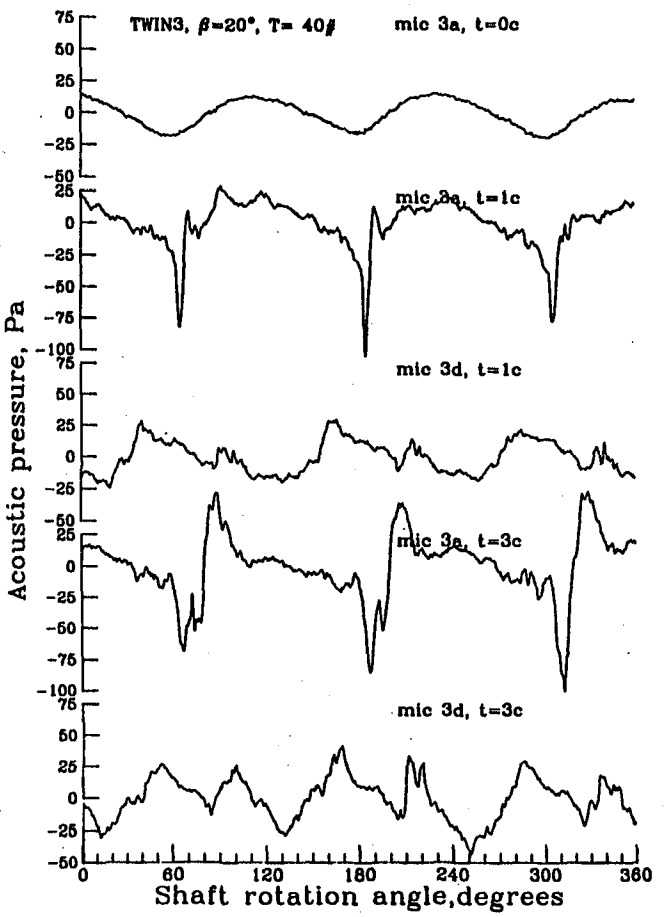

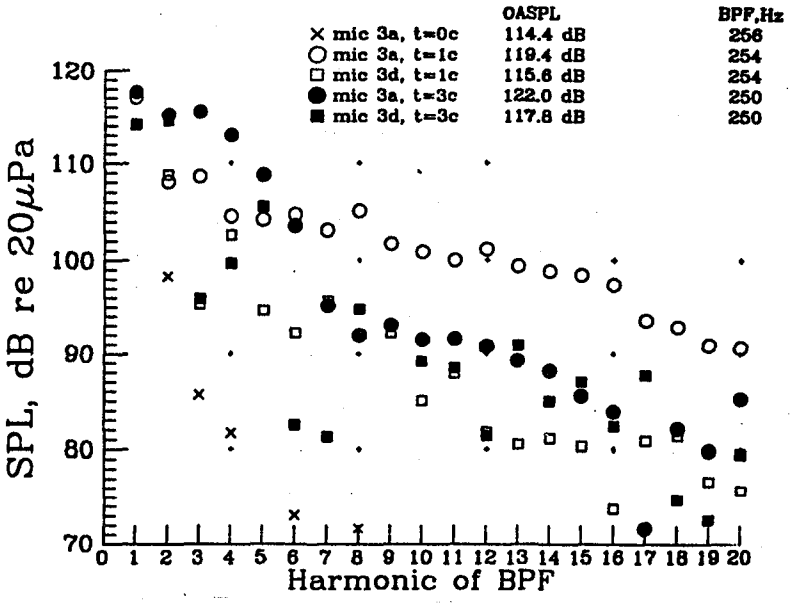

(a) 30° upstream (θ = -30°), microphone 3.

Figure B3.- Noise data for Twin 3, $\beta_{.75}$ = 20°, 40 lbf of thrust.

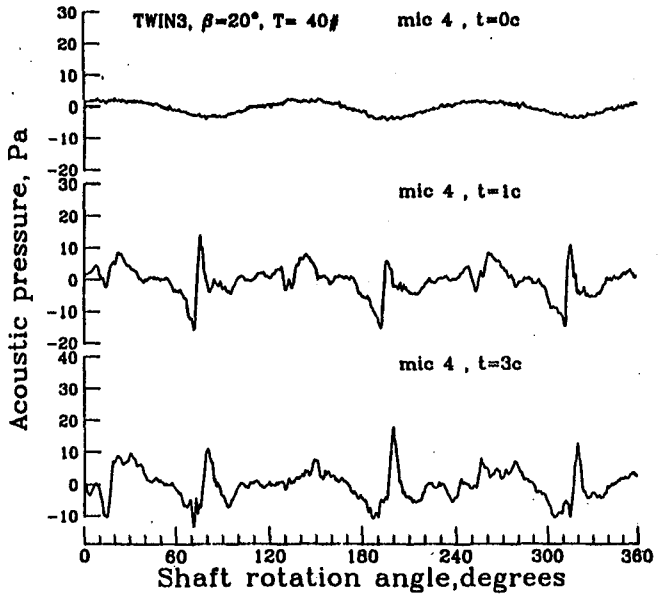

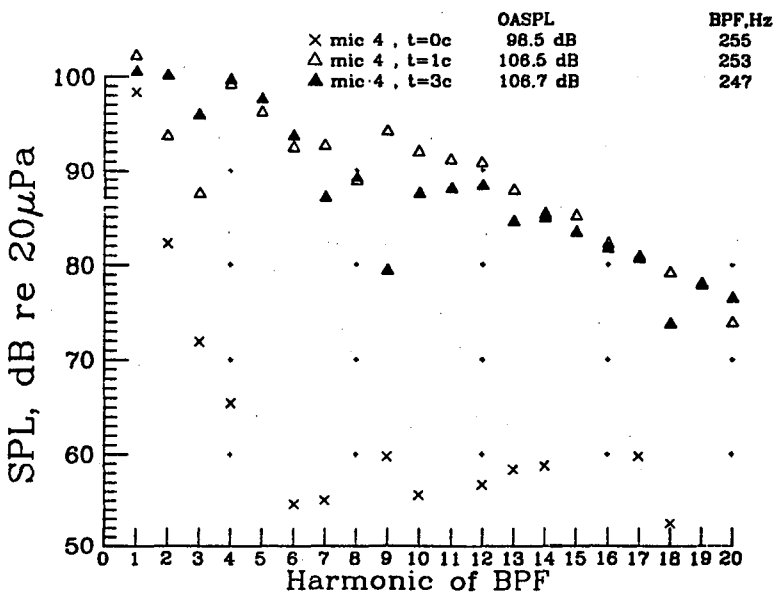

(b) 30° upstream (θ = -30°), microphone 4.

Figure B3.- Continued.

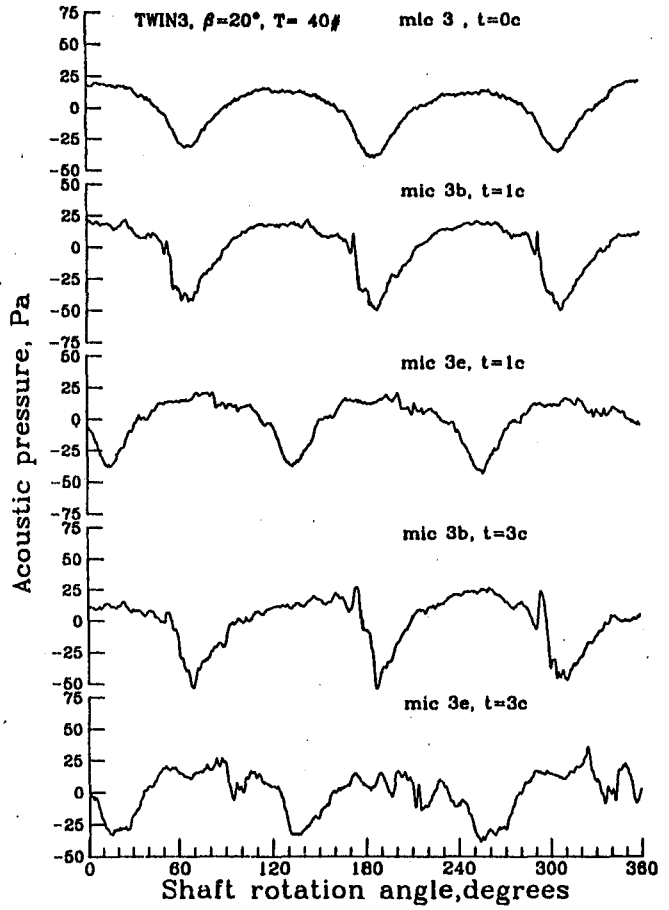

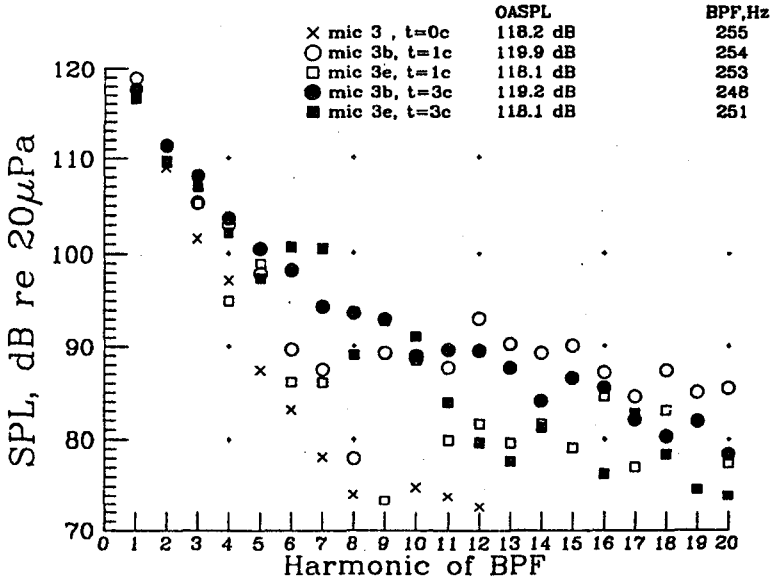

(c) inplane (θ = 0°), microphone 3.

Figure B3.- Continued.

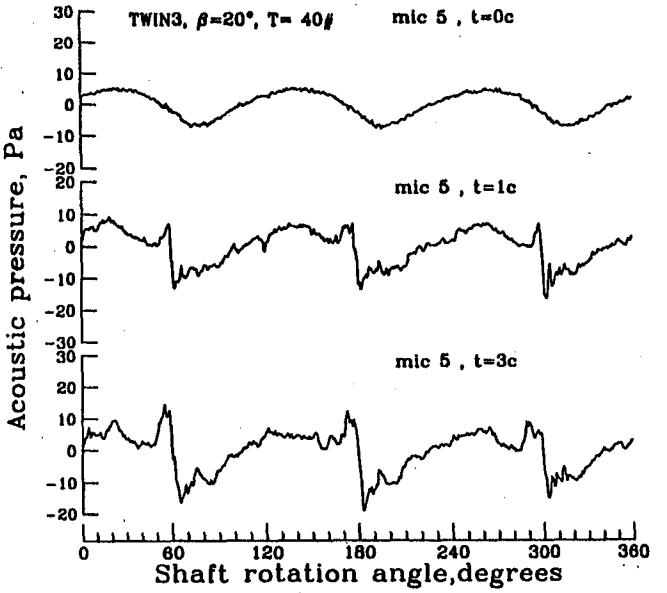

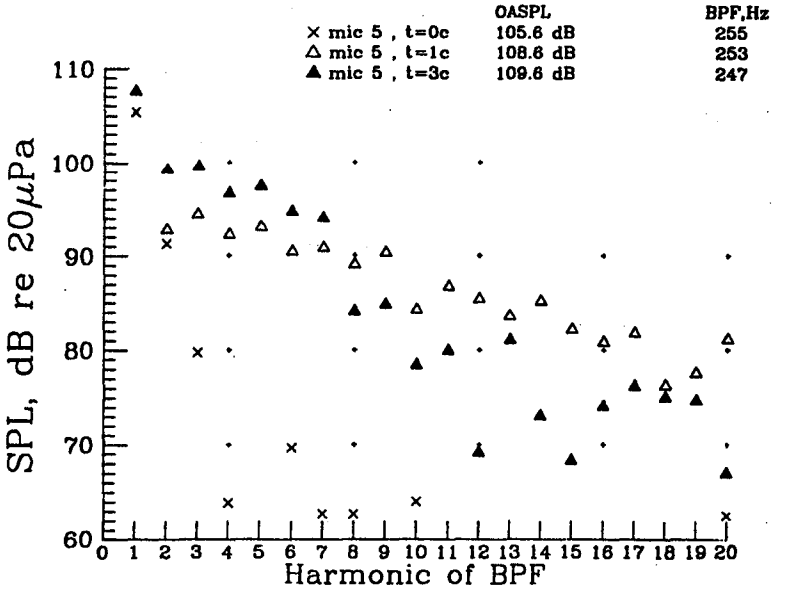

(d) inplane (θ = 0°), microphone 5.

Figure B3.- Continued.

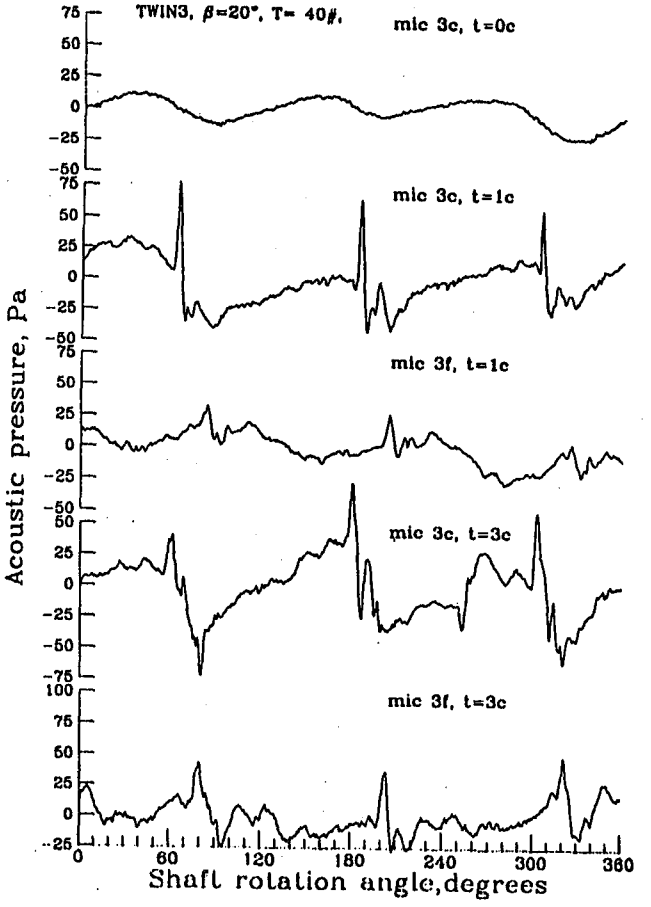

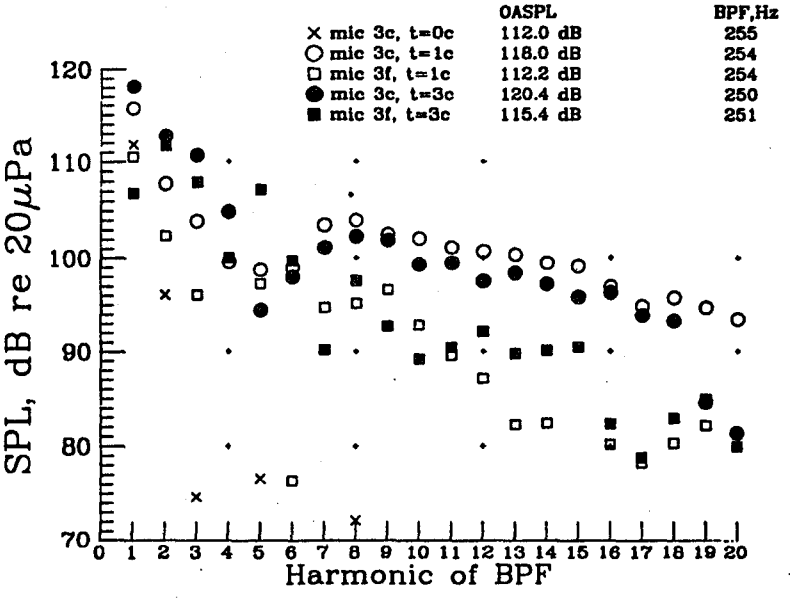

(e) 30° downstream (θ = 30°), microphone 3.

Figure B3.- Continued.

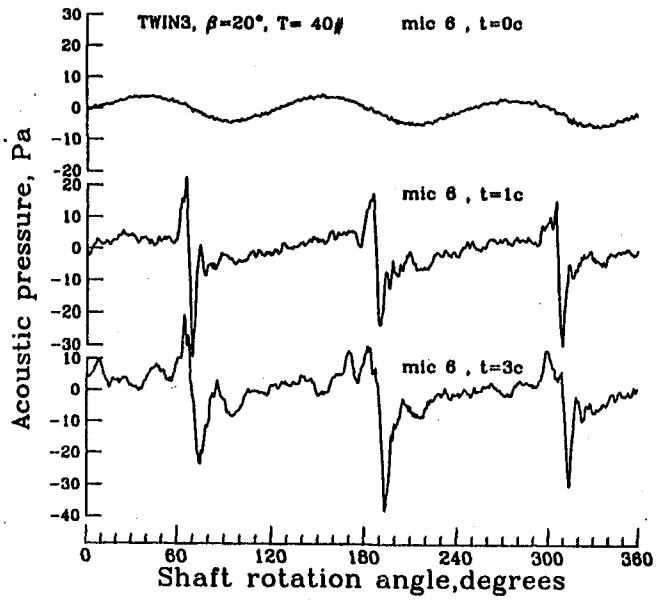

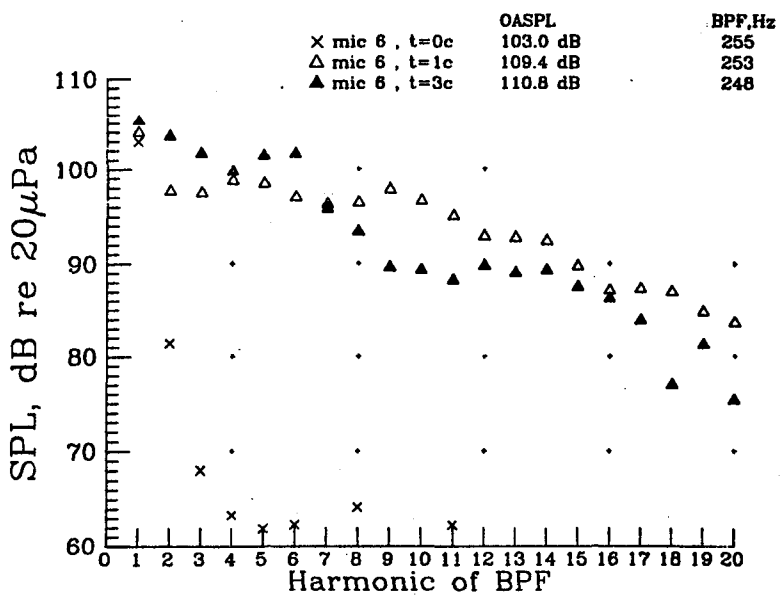

(f) 30° downstream (θ = 30°), microphone 6.

Figure B3.- Concluded.

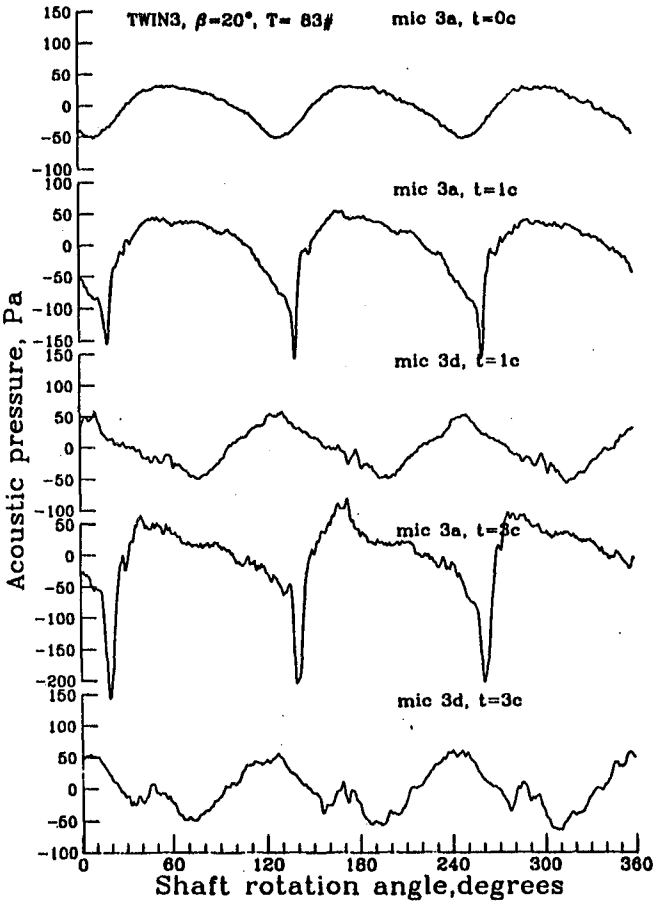

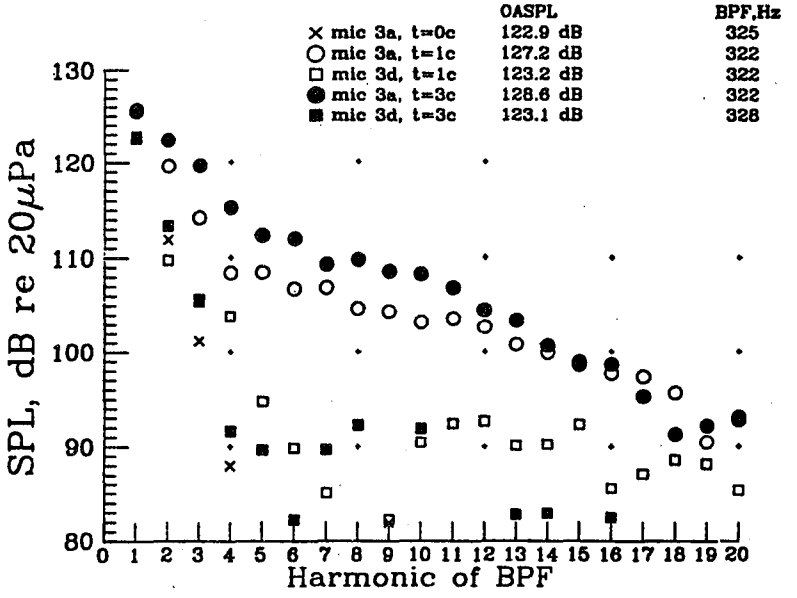

(a) 30° upstream (θ = -30°), microphone 3.

Figure B4.- Noise data for Twin 3, $\beta_{.75}$ = 20°, 83 lbf of thrust.

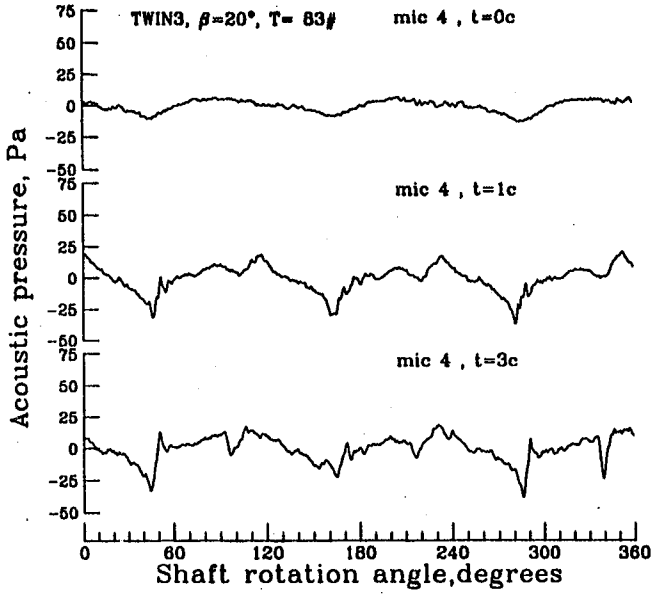

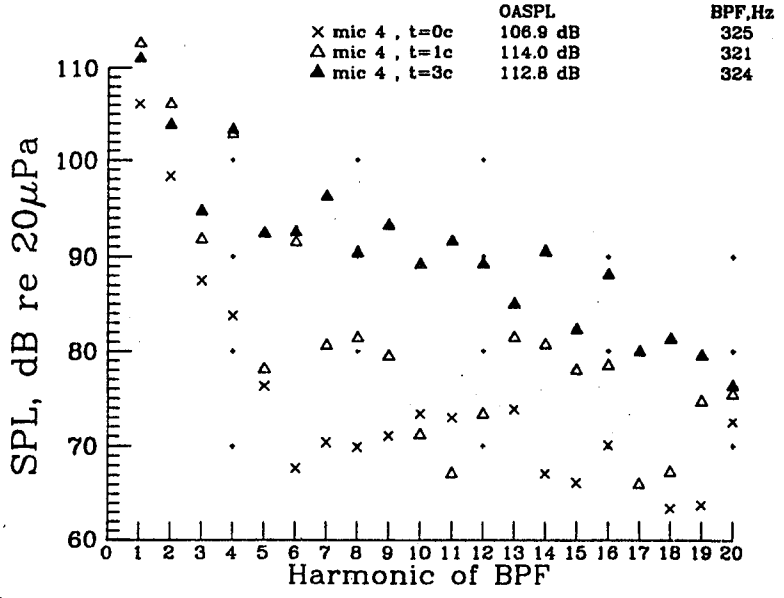

(b) 30° upstream (θ = -30°), microphone 4.

Figure B4.- Continued.

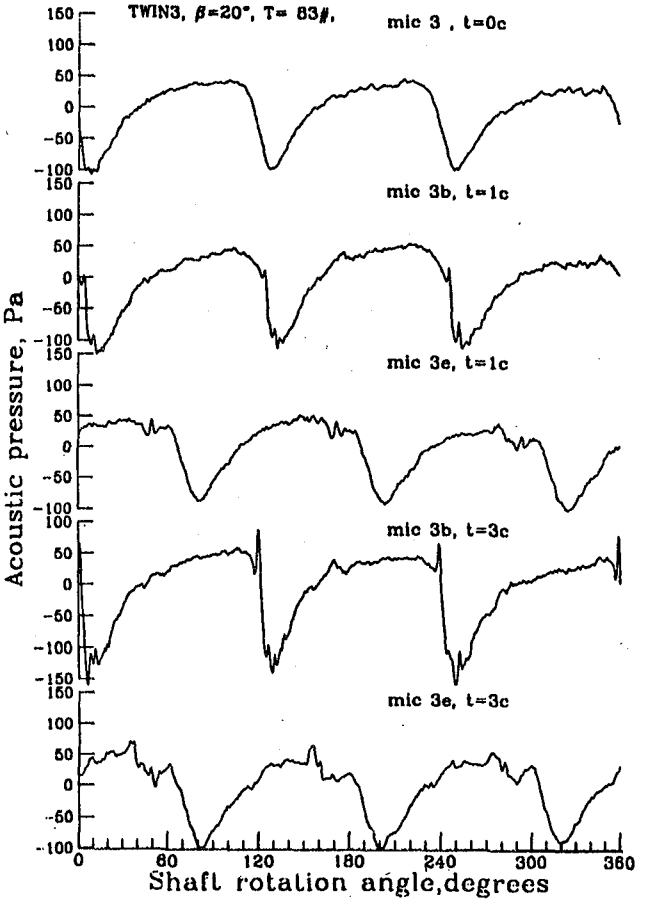

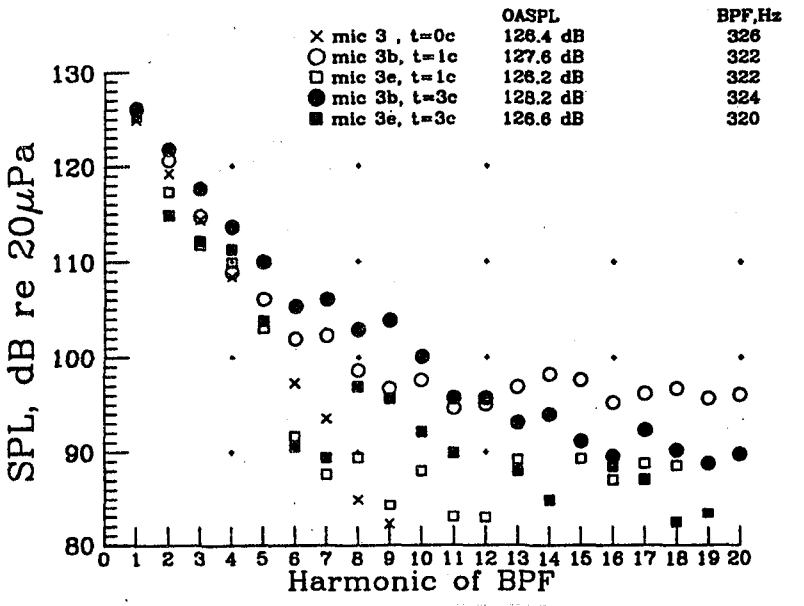

(c) inplane (θ = 0°), microphone 3.

Figure B4.- Continued.

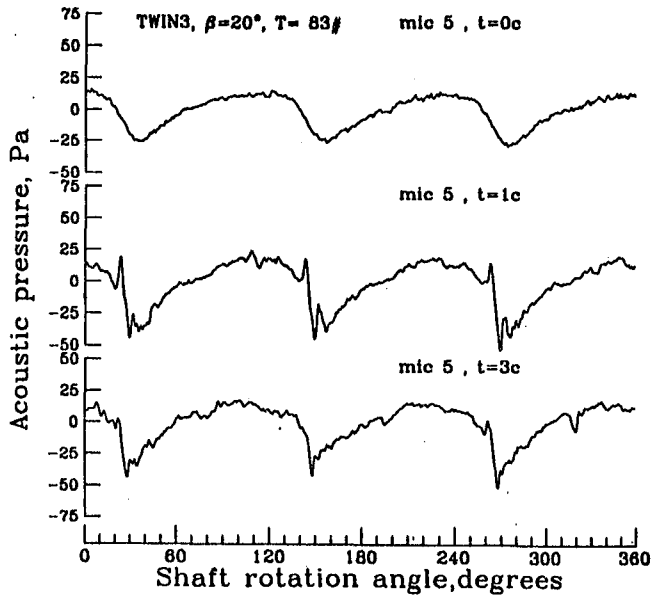

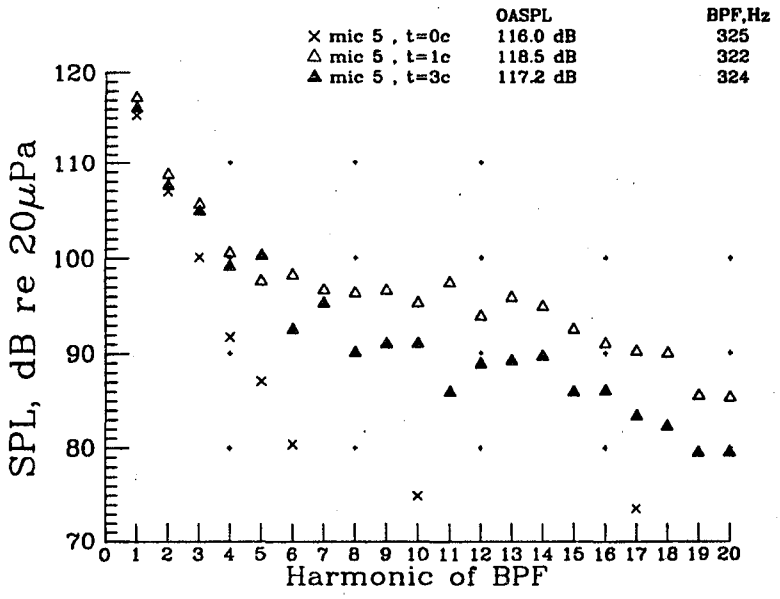

(d) inplane (θ = 0°), microphone 5.

Figure B4.- Continued.

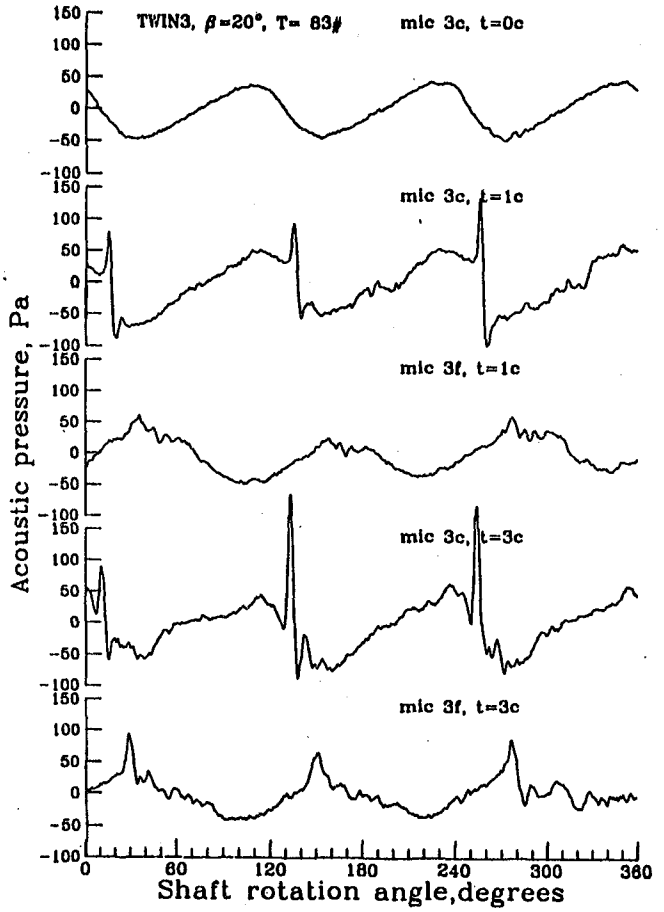

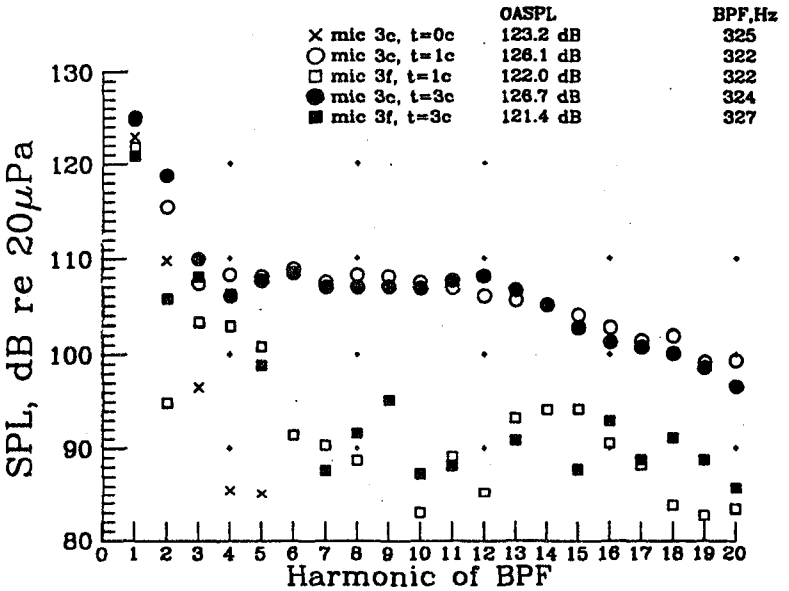

(e) 30° downstream (θ = 30°), microphone 3.

Figure B4.- Continued.

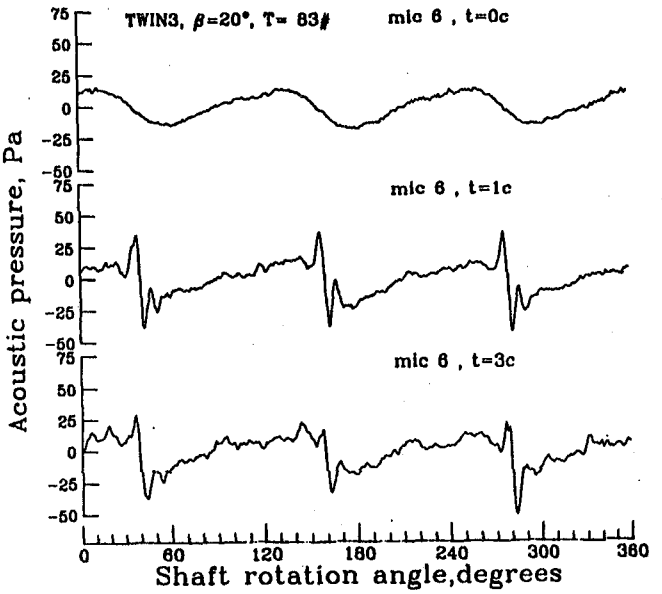

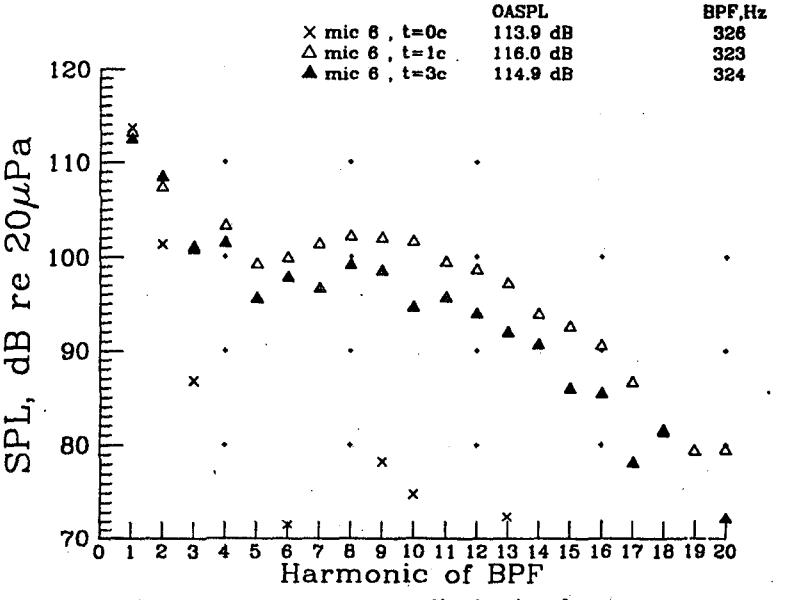

(f) 30° downstream (θ = 30°), microphone 6.

Figure B4.- Concluded.

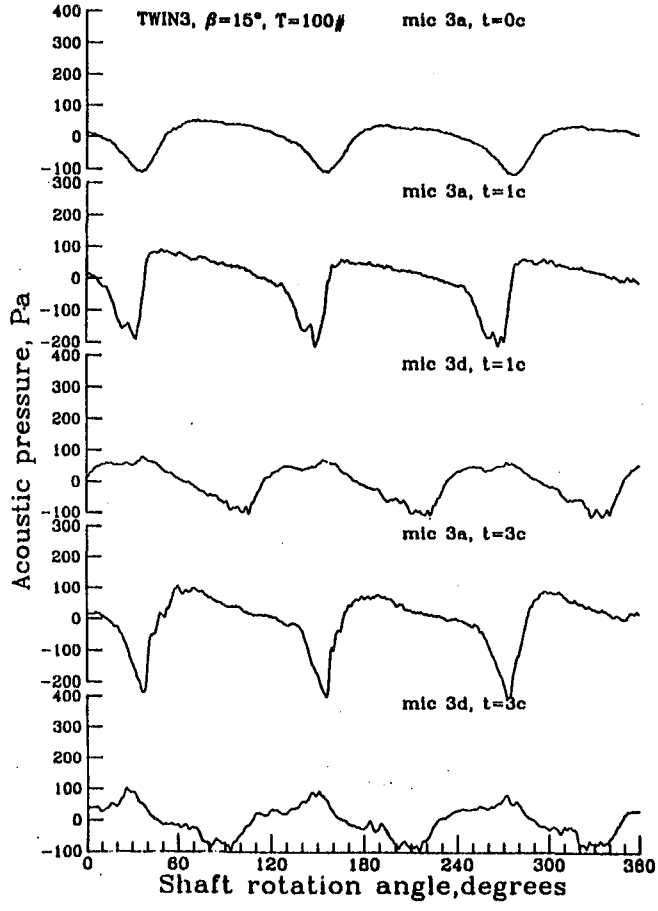

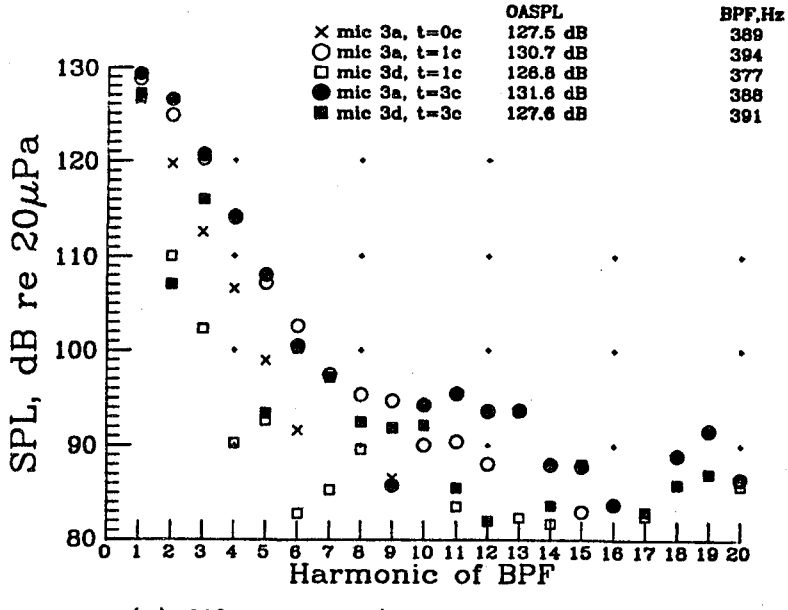

(a) 30° upstream (θ = -30°), microphone 3.

Figure B5.- Noise data for Twin 3, $\beta_{.75}$ = 15°, 100 lbf of thrust.

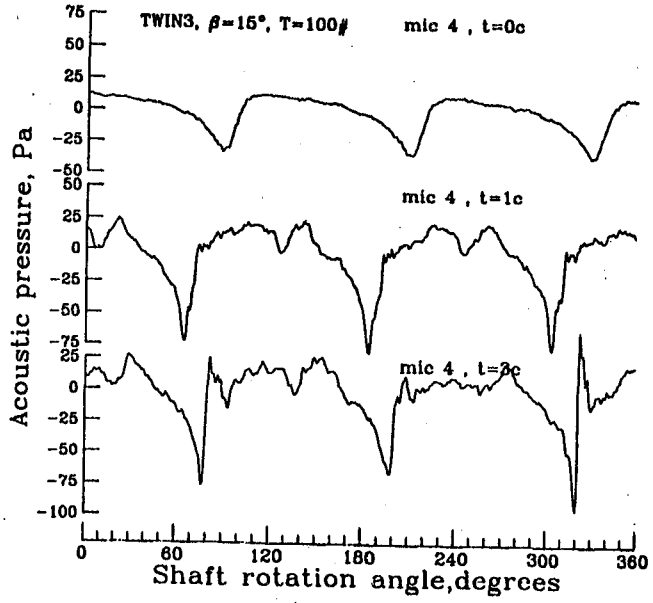

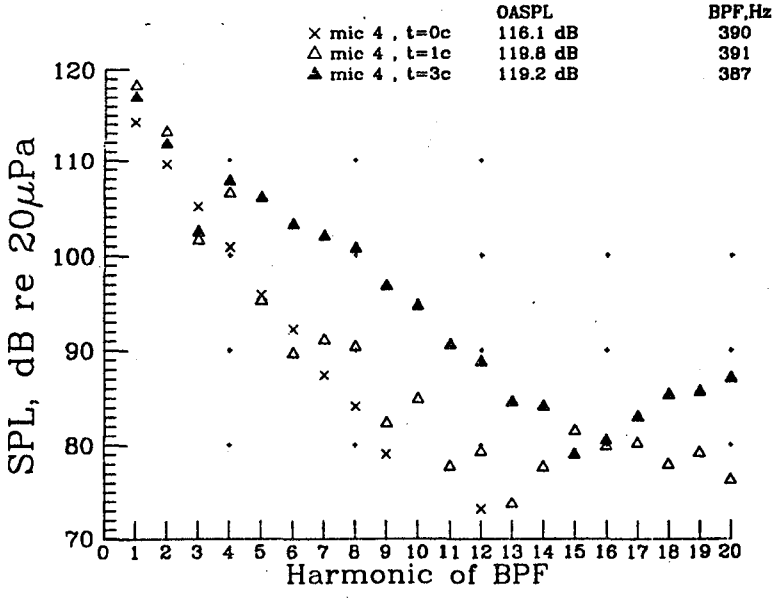

(b) 30° upstream (θ = -30°), microphone 4.

Figure B5.- Continued.

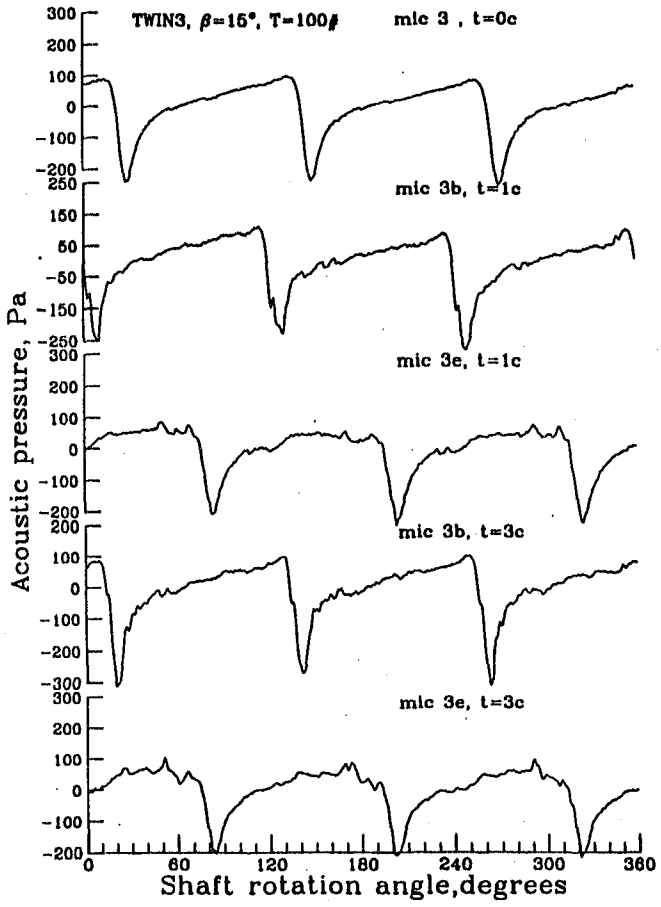

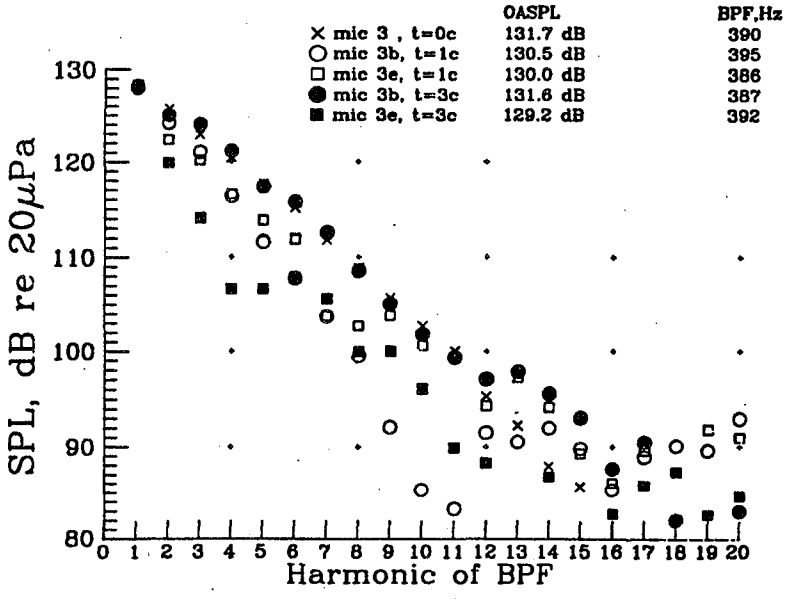

(c) inplane (θ = 0°), microphone 3.

Figure B5.- Continued.

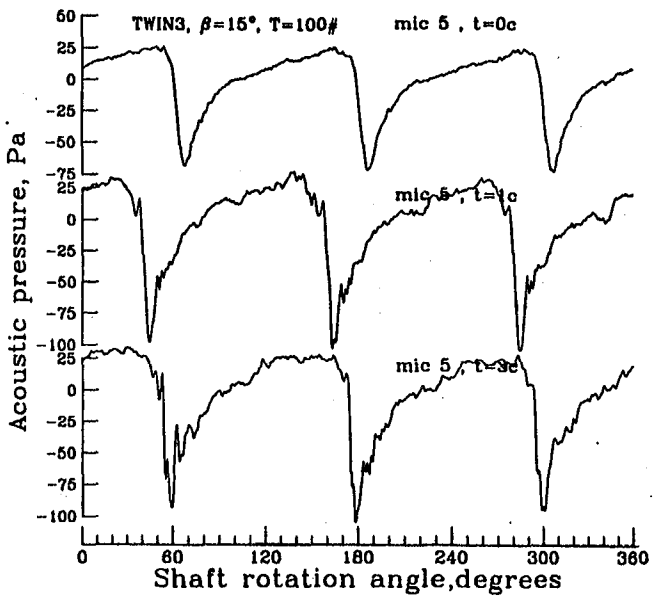

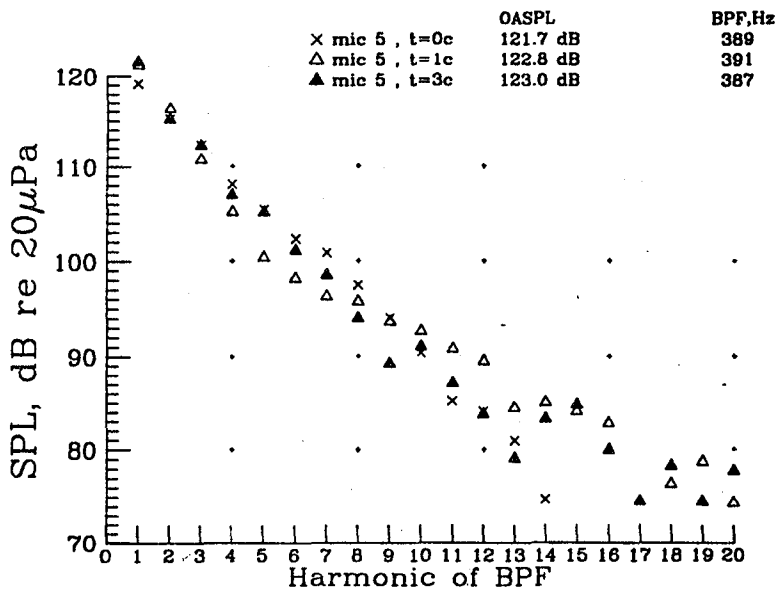

(d) inplane (θ = 0°), microphone 5.

Figure B5.- Continued.

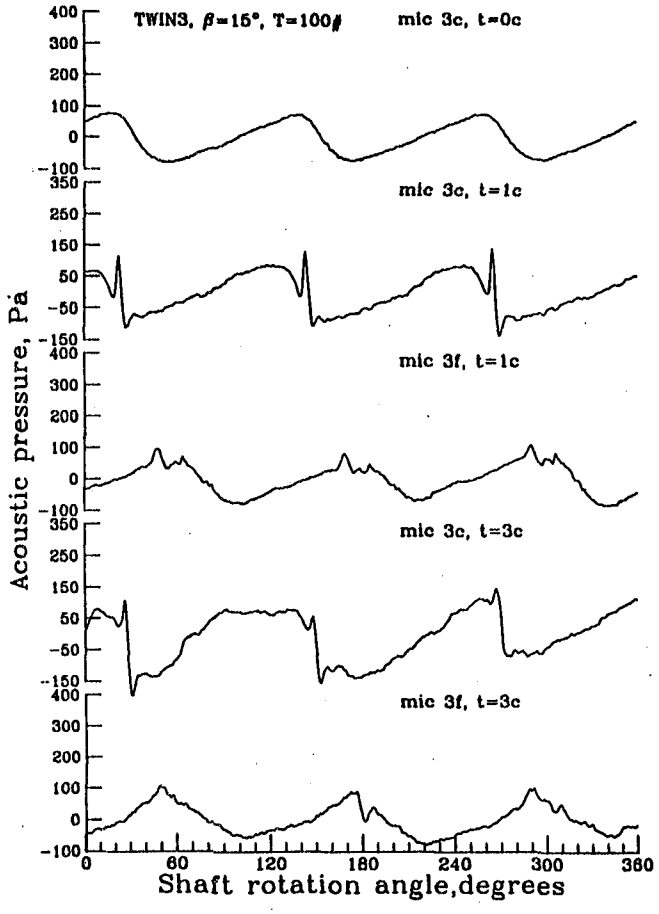

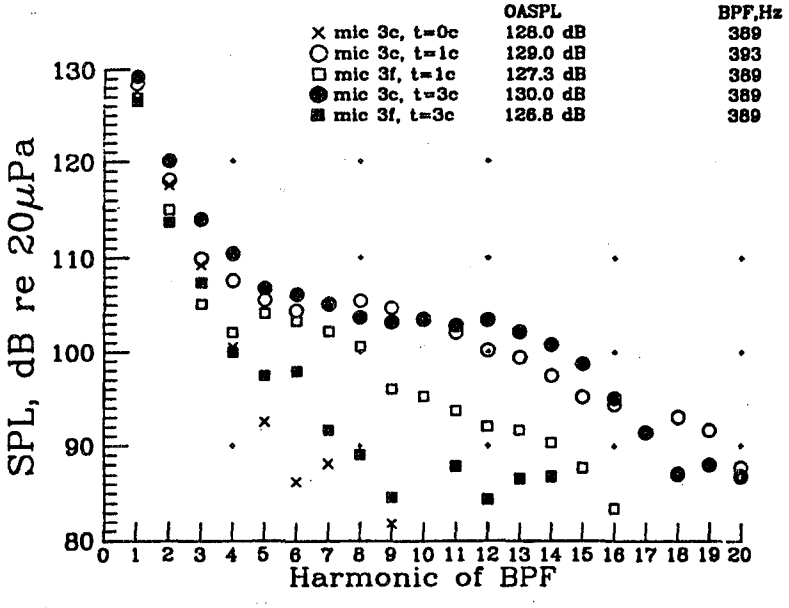

(e) 30° downstream (θ = 30°), microphone 3.

Figure B5.- Continued.

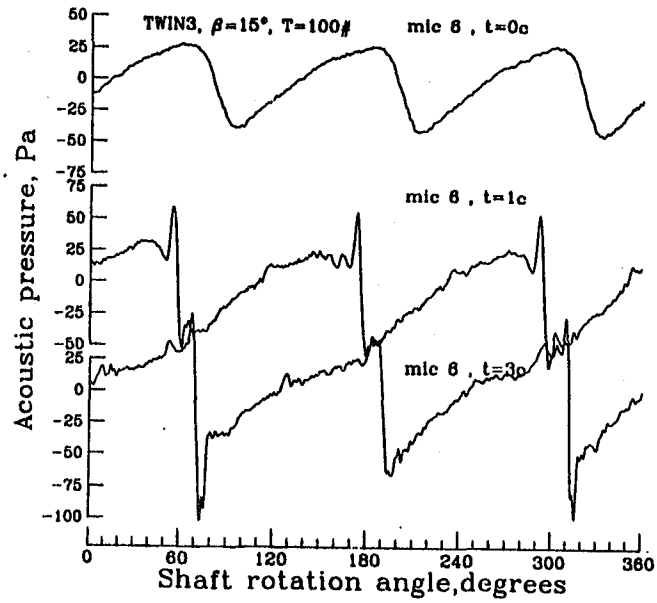

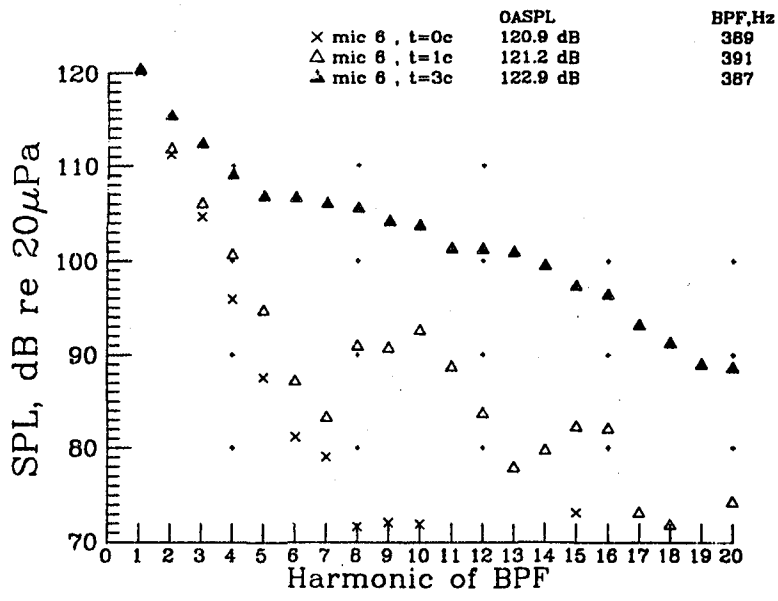

(f) 30° downstream (θ = 30°), microphone 6.

Figure B5.- Concluded.

1. Report No.	2. Government Accession No.	3. Recipient's Catalog No.
NASA TM-85794		

4. Title and Subtitle	5. Report Date
Noise Generated by a Propeller in a Wake	May 1984
	6. Performing Organization Code: 535-03-12-08
7. Author(s): P. J. W. Block	8. Performing Organization Report No.
	10. Work Unit No.
9. Performing Organization Name and Address: NASA Langley Research Center, Hampton, VA 23665	11. Contract or Grant No.
	13. Type of Report and Period Covered: Technical Memorandum
12. Sponsoring Agency Name and Address: National Aeronautics and Space Administration, Washington, DC	14. Sponsoring Agency Code

15. Supplementary Notes

16. Abstract

Propeller performance and noise were measured on two model scale propellers operating in an anechoic flow environment with and without a wake. Wake thickness of one and three propeller chords were generated by an airfoil which spanned the full diameter of the propeller. Noise measurements were made in the relative near field of the propeller at three streamwise and three azimuthal positions. The data show that as much as a 10 dB increase in the OASPL results when a wake is introduced into an operating propeller. Performance data are also presented for completeness.

17. Key Words (Suggested by Author(s))		18. Distribution Statement
Propellers	Aerodynamic Noise	Unclassified - Unlimited
Propeller Noise	Noise Measurement	
Wind Tunnel	Aircraft Wakes	Subject Category 71
Aircraft Noise		

19. Security Classif. (of this report)	20. Security Classif. (of this page)	21. No. of Pages	22. Price*
Unclassified	Unclassified	64	A04

* For sale by the National Technical Information Service, Springfield, Virginia 22161